Tropomyosin-containing Actin Cables Direct the Myo2p-dependent Polarized Delivery of Secretory Vesicles in Budding Yeast

David W. Pruyne, Daniel H. Schott, and Anthony Bretscher

Section of Biochemistry, Molecular and Cell Biology, Cornell University, Ithaca, New York 14853

Abstract. The actin cytoskeleton in budding yeast consists of cortical patches and cables, both of which polarize toward regions of cell growth. Tropomyosin localizes specifically to actin cables and not cortical patches. Upon shifting cells with conditionally defective tropomyosin to restrictive temperatures, actin cables disappear within 1 min and both the unconventional class V myosin Myo2p and the secretory vesicle–associated Rab GTPase Sec4p depolarize rapidly. Bud growth ceases and the mother cell grows isotropically. When returned to permissive temperatures, tropomyosin-containing cables reform within 1 min in polarized arrays. Cable reassembly permits rapid enrichment of Myo2p at the focus of nascent cables as well as the Myo2p-dependent recruitment of Sec4p and the exocyst protein Sec8p, and the initiation of bud emergence. With the loss of actin cables, cortical patches slowly assume an isotropic distribution within the cell and will repolarize only after restoration of cables. Therefore, actin cables respond to polarity cues independently of the overall distribution of cortical patches and are able to directly target the Myo2p-dependent delivery of secretory vesicles and polarization of growth.

Key words: tropomyosin • polarity • actin • MYO2 • SEC4

Polarity is a fundamental property of cells, permitting them to express distinct and specialized surface subdomains (reviewed in Drubin and Nelson, 1996; Keller and Simons, 1997). To generate polarity, cells must target secretion spatially so that lipids and proteins are delivered to specific locations at the plasma membrane. Although in vertebrate cells both microtubules and microfilaments are involved in targeting secretion, in the budding yeast *Saccharomyces cerevisiae* the actin cytoskeleton alone is responsible (reviewed in Bretscher et al., 1994; Finger and Novick, 1998).

Bud growth in yeast requires polarized delivery of secretory vesicles (Thacz and Lampen, 1972; Thacz and Lampen, 1973; Novick and Schekman, 1979; Field and Schekman, 1980). The requirement for microfilaments in this process was first suggested by a correlation between the polarized distribution of actin and the location of cell growth (Adams and Pringle, 1984). Further evidence came with the finding that a conditional defect in actin results in a partial defect in the secretion of invertase (Novick and Botstein, 1985). Subsequently, mutations affecting either actin cytoskeletal components or regulators of actin cytoskeletal polarity were found to be defective in polarized cell growth. For example, defects in the Rho-type GTPase Cdc42p or its exchange factor Cdc24p or in the actin-binding proteins fimbrin (Sac6p) or capping protein (Cap1p, Cap2p) all result in common phenotypes: reduced polarity of the actin cytoskeleton as well as inappropriate growth in the mother rather than in the bud, yielding abnormally large cells (Bender and Pringle, 1989; Adams et al., 1990; Amatruda et al., 1990; Johnson and Pringle, 1990; Adams et al., 1991; Amatruda et al., 1992; Zheng et al., 1993).

Of the five myosins present in the yeast genome, only the unconventional type V myosin encoded by *MYO2* is essential for viability and has been implicated in targeted secretion in yeast (Johnston et al., 1991; Govindan et al., 1995; for review see Brown, 1997). At restrictive temperatures, cells with the conditional *myo2-66* mutation undergo isotropic growth in the mother cell without bud growth or cell division, leading to very large cells, as well as the intracellular accumulation of what appear to be late secretory vesicles. These results were interpreted to suggest that Myo2p is directly responsible for targeting secretory vesicles (Johnston et al., 1991). Although accumulation of vesicles in the *myo2-66* mutant requires a functional secretory pathway, these cells do not accumu-

Address correspondence to Anthony Bretscher, Section of Biochemistry, Molecular and Cell Biology, 353 Biotechnology Building, Cornell University, Ithaca, NY 14853. Tel.: 607-255-5713; Fax: 607-255-2428; E-mail: apb5@cornell.edu

late any of several markers transported by the secretory pathway, suggesting that they accumulate a novel class of secretory vesicle (Liu and Bretscher, 1992; Govindan et al., 1995). However, a role for Myo2p in targeting all post-Golgi secretory vesicles is supported by extensive genetic interactions between *myo2-66* and conditional mutations in genes encoding proteins involved in exocytosis (Govindan et al., 1995). Further, *sec6-4* mutants conditionally defective for all secretion accumulate post-Golgi vesicles in the bud, whereas *sec6-4 myo2-66* double mutants accumulate such vesicles throughout the mother cell and not in the bud (Govindan et al., 1995). These findings indicate that Myo2p targets post-Golgi secretory vesicles to their site of exocytosis and the vesicles that accumulate in the *myo2-66* mutant may represent a novel class especially sensitive to the loss of targeting (Bretscher et al., 1994). However, it is not clear exactly how targeting occurs or how the actin cytoskeleton is involved.

The actin cytoskeleton in yeast is composed of two types of polarized structures: cables and cortical patches. The polarity of both structures parallels the growth of the yeast cell. For example, in cells with a small growing bud, F-actin cables extend from the mother cell into the daughter while F-actin cortical patches are highly enriched within the growing bud. In a variety of cytoskeletal mutants and under a variety of growth conditions, the distribution of these two structures is tightly correlated (Karpova et al., 1998), making a functional dissection of their roles in polarizing the cell difficult. We are interested in the major isoform of yeast tropomyosin, encoded by *TPM1*, as it is a component of actin cables but not cortical patches (Liu and Bretscher, 1989*b*). Yeast *tpm1Δ* cells lack detectable actin cables and have several phenotypes in common with the *myo2-66* mutant. Like the *myo2-66* mutant, *tpm1Δ* cells have partially delocalized cortical patches, a partial defect in polarized growth, and, in some cells, an accumulation of what appear to be post-Golgi secretory vesicles bearing unknown cargo. Furthermore, the *tpm1Δ* and *myo2-66* mutations show synthetic lethality, suggesting that the two gene products participate in targeting secretion (Liu and Bretscher, 1989*b*; Liu and Bretscher, 1992).

We wished to probe the nature of this interaction in more detail, and, in particular, to elucidate whether the polarized actin cables or polarized cortical patches are primary determinants for targeting secretion, as both *tpm1Δ* and *myo2-66* mutants have defects in both actin cable and cortical patch polarity. Specifically, we wished to generate conditional mutants where the short-term effects of the loss of actin cables but not cortical patches could be observed. Actin cables contain actin, fimbrin, and tropomyosin (Tpm1p), but only Tpm1p localizes specifically to cables and not cortical patches. Yeast have two genes encoding tropomyosin, the major isoform encoded by *TPM1* and a minor isoform encoded by *TPM2*. Disruption of *TPM2* alone shows no phenotype, whereas loss of both tropomyosins is lethal (Drees et al., 1995). Therefore, we generated yeast with conditionally defective tropomyosin by isolating temperature-sensitive *tpm1* mutants in a *tpm2Δ* background.

Analysis of one of these conditional *tpm1* mutants has shown that actin cables are highly unstable in the absence of functional tropomyosin and are rapidly restored in its presence. Myo2p-dependent targeting of secretion requires functional cables; Myo2p and secretory proteins polarize extremely rapidly during assembly of tropomyosin-containing actin cables. Moreover, this targeting is independent of the overall distribution of the actin cortical patches, indicating that the overall patch distribution does not establish actin cable polarity or target secretion, but instead requires functional actin cables for its own polarity. These findings reveal that tropomyosin-containing actin cables are required for rapid polarized delivery of secretory vesicles by Myo2p to regions of cell growth.

Materials and Methods

Media, Growth Conditions, and Molecular Genetic Techniques

Standard rich and synthetic media used for growing yeast are described by Sherman (1991). For temperature control experiments, 1-ml culture volumes were transferred to prewarmed or precooled glass tubes for various times, then fixative was added directly to the medium. Yeast transformations were performed using the Frozen-EZ Yeast Transformation Kit (ZYMO Research, Orange, CA) or using a lithium acetate protocol (Ito et al., 1983). *Escherichia coli* strains DH5α and DH10B were used for all bacterial manipulations. Restriction enzymes and T4 DNA ligase (Life Technologies, Inc., Gaithersburg, MD) were used following standard protocols as was *Taq* DNA polymerase (Boehringer Mannheim Corp., Indianapolis, IN), except where described below. Except where noted, primers for PCR were from Life Technologies, Inc.

Generation of Temperature-sensitive tpm1 Alleles

Temperature-sensitive alleles of *TPM1* were generated by mutagenic PCR. The wild-type *TPM1* gene from pRS314 (Sikorski and Hieter, 1989) was amplified (primers: GGGGTCGATGTATAGTCTAAG and GGGGTCGACACATATATCTTACCCG; Cornell Biotechnology Analytical/Synthetic Facility) using conditions favorable for misincorporations, specifically: 50 mM KCl, 10 mM Tris-HCl, 0.5 mM $MnCl_2$, 7 mM $MgCl_2$, 0.2 mM each dGTP and dATP, and 1 mM each dCTP and dTTP (Cadwell and Joyce, 1992). Mutant alleles were transformed into ABY335 (*tpm1Δ tpm2Δ* pRS316[*TPM1*]) by cotransformation of the PCR products with a gapped plasmid (Muhlrad et al., 1992), consisting of pRS314[*TPM1*] linearized with Bpu1102I and StyI. Trp^+ transformants were yeast in which the gapped plasmid (deleted for nucleotides +21 to +488 of *TPM1*) had been repaired by homologous recombination with either PCR-derived *tpm1* or pRS316[*TPM1*], thus transformants carry pRS316[*TPM1*] and pRS314[*tpm1*]. When tested, none showed dominant cold or temperature sensitivity. All clones were then grown on medium containing 5-fluoroorotic acid (United States Biological, Swampscott, MA) to select for the loss of the wild-type pRS316[*TPM1*], leaving pRS314[*tpm1*] as the sole copy of *TPM1*. Surviving clones were screened for recessive temperature and cold sensitivity: of 594 Trp^+ transformants, 215 were 5-fluoroorotic acid resistant, and two of those were recessively temperature sensitive (alleles *tpm1-1* and *tpm1-2*) while none were cold sensitive. The *tpm1-1* and *tpm1-2* coding regions were recloned into ABY335 to verify that the conditional mutations were in the coding region. They were then sequenced (Cornell University Biotechnology Resource Center). Resultant strains were ABY932 (*tpm1Δ tpm2Δ* pRS314[*tpm1-1*]) and ABY933 (*tpm1Δ tpm2Δ* pRS314[*tpm1-2*]).

Construction of Yeast Strains

The genotypes of all yeast strains used in this study are described in Table I. Strains with genomic *tpm1-2 tpm2Δ* were generated in the following manner: *TPM1* in a plasmid-borne 2.2-kb genomic insert (Liu and Bretscher, 1989*b*) was digested with Bpu1102I/StyI to replace bases +21 through +488 with that region of *tpm1-2*. *LEU2* was amplified by PCR from pRS315 (Sikorski and Hieter, 1989) to introduce flanking NheI sites (oligonucleotide primers GGGCTAGCGTGGTAAGGCCGT and GGGCTAGCGGTCGAGGAGAAC), then cloned into an NheI site at position −236 relative to *tpm1-2*. The *tpm1-2::LEU2* insert was released by digestion with Alw26I/BcgI and transformed into ABY946 (*TPM1*

Table I. Strains Used

Strain	Genotype	Source
ABY335	*MATα tpm1Δ::LEU2 tpm2Δ::HIS3 his3Δ-200 leu2-3,112 lys2-801 trp1-1 ura3-52 [URA3::TPM1]*	This study
ABY703	*MATα sec6-4 his3Δ-200 leu2-3,112 lys2-801 trp1-1 ura3-52*	Harsay and Bretscher (1995)
ABY913	*MATa ade2-101 ade3 his7 leu2-3,112 trp1-1 ura3-52* *MATα ade2-101 ade3 his7 leu2-3,112 trp1-1 ura3-52*	This study
ABY932	*MATα tpm1Δ::LEU2 tpm2Δ::HIS3 his3Δ-200 leu2-3,112 lys2-801 trp1-1 ura3-52 [TRP1::tpm1-1]*	This study
ABY933	*MATα tpm1Δ::LEU2 tpm2Δ::HIS3 his3Δ-200 leu2-3,112 lys2-801 trp1-1 ura3-52 [TRP1::tpm1-2]*	This study
ABY944	*MATa tpm1-2::LEU2 tpm2Δ::HIS3 his3Δ-200 leu2-3,112 lys2-801 trp1-1 ura3-52*	This study
ABY945	*MATa tpm2Δ::HIS3 his3Δ-200 leu2-3,112 lys2-801 trp1-1 ura3-52*	This study
ABY946	*MATα tpm2Δ::HIS3 his3Δ-200 leu2-3,112 lys2-801 trp1-1 ura3-52*	This study
ABY950	*MATa tpm1-1::LEU2 tpm2Δ::HIS3 his3Δ-200 leu2-3,112 lys2-801 trp1-1 ura3-52*	This study
ABY971	*MATa tpm1-2::LEU2 tpm2Δ::HIS3 his3Δ-200 leu2-3,112 lys2-801 trp1-1 ura3-52* *MATα tpm1-2::LEU2 tpm2Δ::HIS3 his3Δ-200 leu2-3,112 lys2-801 trp1-1 ura3-52*	This study
ABY973	*MATa tpm2Δ::HIS3 his3Δ-200 leu2-3,112 lys2-801 trp1-1 ura3-52* *MATα tpm2Δ::HIS3 his3Δ-200 leu2-3,112 lys2-801 trp1-1 ura3-52*	This study
ABY987	*MATa tpm2Δ::HIS3 SEC8:HA3::TRP1 his3Δ-200 leu2-3,112 lys2-801 trp1-1 ura3-52* *MATα tpm2Δ::HIS3 SEC8:HA3::TRP1 his3Δ-200 leu2-3,112 lys2-801 trp1-1 ura3-52*	This study
ABY988	*MATa tpm1-2::LEU2 tpm2Δ::HIS3 SEC8:HA3::TRP1 his3Δ-200 leu2-3,112 lys2-801 trp1-1 ura3-52* *MATα tpm1-2::LEU2 tpm2Δ::HIS3 SEC8:HA3::TRP1 his3Δ-200 leu2-3,112 lys2-801 trp1-1 ura3-52*	This study
ABY989	*MATa tpm2Δ::HIS3 MYO5:HA3::TRP1 his3Δ-200 leu2-3,112 lys2-801 trp1-1 ura3-52* *MATα tpm2Δ::HIS3 MYO5:HA3::TRP1 his3Δ-200 leu2-3,112 lys2-801 trp1-1 ura3-52*	This study
ABY990	*MATa tpm1-2::LEU2 tpm2Δ::HIS3 MYO5:HA3::TRP1 his3Δ-200 leu2-3,112 lys2-801 trp1-1 ura3-52* *MATα tpm1-2::LEU2 tpm2Δ::HIS3 MYO5:HA3::TRP1 his3Δ-200 leu2-3,112 lys2-801 trp1-1 ura3-52*	This study
ABY991	*MATa tpm2Δ::HIS3 cap2::TRP1::GFP:CAP2 his3Δ-200 leu2-3,112 lys2-801 trp1-1 ura3-52* *MATα tpm2Δ::HIS3 cap2::URA3::GFP:CAP2 his3Δ-200 leu2-3,112 lys2-801 trp1-1 ura3-52*	This study
ABY992	*MATa tpm1-2::LEU2 tpm2Δ::HIS3 cap2::TRP1::GFP:CAP2 his3Δ-200 leu2-3,112 lys2-801 trp1-1 ura3-52* *MATα tpm1-2::LEU2 tpm2Δ::HIS3 cap2::URA3::GFP:CAP2 his3Δ-200 leu2-3,112 lys2-801 trp1-1 ura3-52*	This study
ABY999	*MATa sec6-4 tpm1-2::LEU2 tpm2Δ::HIS3 SEC8:HA3::TRP1 his3Δ-200 leu2-3,112 lys2-801 trp1-1 ura3-52* *MATα sec6-4 tpm1-2::LEU2 tpm2Δ::HIS3 SEC8:HA3::TRP1 his3Δ-200 leu2-3,112 lys2-801 trp1-1 ura3-52*	This study
ABY1100	*MATa myo2-66 tpm1-2::LEU2 tpm2Δ::HIS3 SEC8:HA3::TRP1 his3Δ-200 leu2-3,112 lys2-801 trp1-1 ura3-52*	This study
NY1396	*MATa myo2-66 leu2-3,112::LEU2::SEC8:3x-c-myc ura3-52*	P. Novick

tpm2Δ) to replace *TPM1* with *tpm1-2::LEU2*. Integration of *tpm1-2* into Leu$^+$ transformants was verified by testing for temperature sensitivity and sequencing the *tpm1* locus. The resultant strain is ABY944 (*tpm1-2 tpm2Δ*). Homozygous diploids ABY971 (*tpm1-2/tpm1-2 tpm2Δ/tpm2Δ*) and ABY973 (*TPM1/TPM1 tpm2Δ/tpm2Δ*) were generated through backcrossing ABY944 to ABY945, sporulating the heterozygous diploid, and remating appropriate spores. ABY950 (*tpm1-1 tpm2Δ*) was generated in the same way.

A hemagglutinin (HA)[1] epitope-tagged *MYO5* allele, (*MYO5:HA3*) was introduced into the ABY971 and 973 backgrounds in the following manner: PCR amplification of the plasmid pCS124 (a gift from Caroline Shamu, Harvard Medical School, Boston, MA) using primers having homology to the 3′ end of *MYO5* (TAGAGAGTGATGACGAGGAGGCTAACGAAGATGAAGAGGAAGATGATTGGGTATTCACCATGGCCTACCC and TACTCTATTTGCTCGTATAGAGTATATACTCGCTAAATACATTTTGATTATGGTGCACTCTCAGTACAAT) yielded linear DNA that upon transformation into yeast converts *MYO5* into *MYO5:HA3::TRP1*. Trp$^+$ transformants of ABY971 were verified for production of tagged Myo5p by Western analysis using anti-HA monoclonal 12CA5 (Boehringer Mannheim Corp.). The resultant heterozygous diploid was sporulated and appropriate spores remated to generate homozygous *MYO5:HA3/MYO5:HA3* in the ABY971 background (ABY990) or crossed to ABY945 and again sporulated and backcrossed to generate *MYO5:HA3* homozygous in a *TPM1* background (ABY989).

SEC8:HA3 allele was introduced in the same manner, using primers with homology to the 3′ end of *SEC8* (TTGGAAAACTTAAAAGCAAATTGAATGCTGTCCATACTGCAAACGAAAAAGTATTCACCATGGCCTACCC and TTTTCATTCATTTATTTATCAAATTATTTTTTACACAAACTAAAAATGTCATGGTGCACTCTCAGTACAAT), resulting in homozygous *SEC8:HA3::TRP1* in the ABY973 and ABY971 backgrounds (ABY987 and ABY988, respectively).

A green fluorescent protein-tagged *CAP2* allele (*GFP:CAP2*) was introduced using a modified version of plasmid pBJ646 (Waddle et al., 1996), kindly donated by J. Cooper (Washington University School of Medicine, St. Louis, MO). A PstI/EcoRV fragment from pBJ646 was cloned into either pRS304 or pRS306 (Sikorski and Hieter, 1989), yielding pDP122 and pDP124, respectively. Linearization of either plasmid with EcoRI yields DNA competent to replace the endogenous *CAP2* allele with *cap2* with the terminal 31 residues replaced with 52 residues derived from the plasmid multiple cloning site, followed by a stop, then either *TRP1* or *URA3,* and, finally, *GFP:CAP2* behind the *CAP2* promoter. In short, transformants bear either *cap2::TRP1::GFP:CAP2* or *cap2::URA3::GFP:CAP2*. Both alleles were transformed into ABY971 and ABY973 to generate homozygous *tpm1-2/tpm1-2 tpm2Δ/tpm2Δ GFP:CAP2/GFP:CAP2* (ABY992) and *TPM1/TPM1 tpm2Δ/tpm2Δ GFP:CAP2/GFP:CAP2* (ABY991), respectively.

Triple mutant *myo2-66 tpm1-2 tpm2Δ* was generated in two steps. First, ABY946 (*tpm2Δ::HIS3*) was crossed to NY1396 (*myo2-66*), then sporulated to isolate *myo2-66 tpm2Δ*. This was then crossed to a clone bearing *tpm1-2 tpm2Δ SEC8:HA3::TRP1* and the diploid sporulated to isolate *myo2-66 tpm1-2 tpm2Δ SEC8:HA3* (ABY1100). Triple mutant *sec6-4 tpm1-2 tpm2Δ* was generated by the same procedure except using the initial strains ABY945 (*tpm2Δ*) and ABY703 (*sec6-4*) and as a final step, crossing two haploid *sec6-4 tpm1-2 tpm2Δ SEC8:HA3* spores to generate the homozygous diploid (ABY999).

Affinity Purification of Antibodies to Tpm1p, Tpm2p, and Myo2p

Tpm2p-specific antibodies were prepared from crude rabbit antiserum B43 that recognizes both Tpm1p and Tpm2p (Drees et al., 1995). Tpm2p was purified as described (Drees et al., 1995) and 2.8 mg coupled to CNBr-activated Sepharose 4B (Sigma Chemical Co., St. Louis, MO). Tpm1p was purified as described (Liu and Bretscher, 1989*a*) and 1.5 mg coupled to CNBr-coupled Sepharose 4B. Tpm2p-specific antibodies were

1. *Abbreviations used in this paper:* DIC, differential interference contrast; GFP, green fluorescent protein; HA, hemagglutinin.

generated by affinity purification of B43 against coupled Tpm2p followed by immunodepletion by coupled Tpm1p. Affinity pure Tpm1p-specific antibodies were prepared from either crude rabbit antiserum 138 (Liu and Bretscher, 1989*a*) or from IgY yolk preparation C37 (from yolks from chickens immunized with Tpm1p, as described by Gassmann et al., 1990). Antibodies for Myo2p were raised in rabbits immunized with recombinant peptide encompassing residues 784–1118 of Myo2p (the IQ–repeats and coiled–coil region), then affinity purified with coupled recombinant peptide.

Light Microscopy and Imaging

Immunofluorescence and fluorescence microscopy were performed as described by Pringle et al. (1989). Staining with anti-Act1p, -Tpm1p, -Tpm2p, and -Myo2p was done after MeOH/acetone postfixation (Pringle et al., 1989), whereas staining with anti-Sec4p or anti-HA was after 5 min of postfixation in 0.1% SDS in PBS, followed by 10 washes in PBS. For double-labeling with anti-Sec4p and anti-Tpm1p, with anti-Sec4p and anti-Myo2p, or with anti-Myo2p and 12CA5, cells were postfixed for 30 s in −20°C acetone, dried, then incubated for 5 min in 0.025% SDS/PBS followed by 10 washes in PBS. Double-labeling with rhodamine-phalloidin and anti-Tpm1p or with rhodamine-phalloidin and anti-Myo2p were after postfixation for 30 s in −20°C acetone. All cells were blocked 30 min in PBS/BSA. Antibody dilutions into PBS/BSA were: anti-Act1p (1:25), rabbit anti-Tpm1p (1:50), chicken anti-Tpm1p (1:100), anti-Tpm2p (1:100), anti-Myo2p (1:20), C.1.2.3. (anti-Sec4p [Walch-Solimena et al., 1997]; 1:50; kindly donated by P. Novick [Yale University School of Medicine, New Haven, CT]), 12CA5 (anti-HA; 1:75; Boehringer Mannheim Corp.), goat anti–rabbit IgG FITC (1:75; ICN Biochemicals, Inc., Aurora, OH), goat anti–rabbit IgG TRITC (1:100; ICN Biochemicals, Inc.), goat anti–mouse IgG FITC (1:300; Organon Teknika Corp., West Chester, PA), and donkey anti–chicken IgY TRITC (1:250; Jackson ImmunoResearch Laboratories, Inc., West Grove, PA). Incubations were for 1.5 h at room temperature for primary antibodies and 1 h at room temperature for secondary antibodies. All secondaries were preincubated with fixed spheroplasts for 1 h at room temperature before use. Staining of actin with rhodamine-phalloidin (Molecular Probes, Eugene, OR), DNA with 4′, 6′-diamidino-2-phenylidole dihydrochloride (Sigma Chemical Co.), and chitin with calcofluor (Sigma Chemical Co.) were performed as described by Pringle et al. (1989). Fluid-phase endocytosis was assayed as described by Riezman (1985) using Lucifer yellow CH (Molecular Probes).

Live cells were placed under 2% agarose in synthetic medium, with appropriate amino acids, in a ΔT dish (Bioptechs, Inc., Butler, PA) and visualized using differential interference contrast (DIC) microscopy. Temperature was controlled using a ΔT dish and objective controllers, stage adaptor, and objective heater (Bioptechs, Inc.). Live cells expressing GFPCap2p were washed with water and placed under 2% agarose in nonfluorescent synthetic medium for observation (Waddle et al., 1996).

DIC and fluorescence images were acquired by a RTC/CCD digital camera (Princeton Instruments, Inc., Trenton, NJ) using a Zeiss Axiovert 100 TV microscope (Carl Zeiss, Inc., Oberkochen, Germany) and then processed using the Metamorph Imaging System (Universal Imaging Corp., West Chester, PA). Photographs of Western blots were acquired through FOTO/Analyst Archiver (FOTODYNE Inc., Hartland, WI). All digital images were processed through Adobe Photoshop 3.0 (Adobe Systems, Inc., Mountain View, CA).

Electron Microscopy

Intracellular membranes were visualized by electron microscopy of cells prepared using the permanganate fixation procedure (Kaiser and Schekman, 1990). 50-ml cultures of cells (OD_{600} = 0.4) were grown under described conditions and fixed for 10 min by direct addition of 10-fold concentrated fixative 20% glutaraldehyde (EM grade; Electron Microscopy Sciences, Fort Washington, PA), 20% formaldehyde (EM grade; Electron Microscopy Sciences), 0.4 M KPi (pH 6.7), then pelleted gently (700 rpm, 5 min) and resuspended in fixative for 1 h at room temperature. Cells were then washed five times with water, resuspended in 5 ml prefiltered 4% aqueous $KMnO_4$, and incubated for 2 h at 8°C. Cells were then washed 10 times with water, resuspended in 10 ml 1% aqueous uranyl acetate, and incubated for 16 h at 8°C in the dark. These were then washed five times with water, dehydrated in graded ethanol (50, 70, 80, 85, 90, 95, and 3 × 100%), and embedded in Spurr resin (Polysciences, Inc., Warrington, PA): 1 h in 2:1 EtOH/resin, 2.5 h in 1:1 EtOH/resin, overnight in 1:1 EtOH/resin (permitting evaporation of EtOH), 2 h in 100% resin, followed by overnight baking at 65°C. Hardened samples were thin-sectioned, and pale gold sections were mounted on 300 hex mesh copper grids and stained for 1 min in Reynold's lead citrate (Dykstra, 1993). Sections were viewed and photographed in a Phillips-301 electron microscope at 60 kV, using SO-163 film.

Other Procedures

SDS-PAGE was performed as described by Laemmli (1970). For probing of internal and external Bgl2p, yeast were fractionated into internal and external proteins. In brief, yeast were killed by addition of 40 mM NaF and 10 mM NaN_3, washed twice in the same, and converted to spheroplasts (1.4 M sorbitol, 25 mM KPi, pH 7.5, 25 mM β-mercaptoethanol, 5 mM NaN_3, 20 mM NaF, 25 μg/ml zymolyase; ICN Immunobiologicals, Lisle, IL) for 1 h at 37°C. Spheroplasts were centrifuged to separate internal protein from external protein. Denaturing sample buffer was added to both fractions. All other cell extracts for Western analysis were prepared as described by Horvath and Riezman (1994). After electrophoresis, proteins were transferred by electroelution to nitrocellulose (Schleicher and Schuell, Keene, NH) and blocked with 10% milk for 30 min. Incubations with primary and secondary antibodies were all for 1 h at room temperature at the following dilutions: anti-Bgl2p (1:10,000; Mrsa et al., 1993), 12CA5 (1:1,000; Boehringer Mannheim Corp.), B43 (anti-Tpm1p/Tpm2p, 1:2,000; Drees et al., 1995), anti-Tpm2p (1:100), anti-Tpm1p (1:200), HRP-conjugated goat anti–rabbit IgG (1:10,000; Organon Teknika Corp.), and HRP-conjugated goat anti–mouse IgG (1:5,000; Life Technologies, Inc.), all in the presence of 1% milk in rinse buffer. Blots were visualized using an enhanced chemiluminescent kit (Amersham Life Science, Little Chalfont, United Kingdom). To assay invertase secretion, invertase was induced as described by Ballou (1990) and cells were fractionated as described above into internal and external proteins, with the exception that nondenaturing sample buffer was added to fractions before loading for electrophoresis in a 7.25% native acrylamide gel. Invertase activity was detected within the gel as described (Ballou, 1990).

Results

Tpm2p, Like Tpm1p, Localizes to Actin Cables in Wild-Type Cells and to Regions of Cell Growth in *tpm1Δ* Cells

Tpm1p specifically localizes to actin cables. To determine whether this is a common, and possibly essential, feature of tropomyosins in yeast, we examined the localization of the minor tropomyosin isoform, Tpm2p, in both wild-type and *tpm1Δ* cells. Although Tpm1p and Tpm2p are 64.5% identical in primary sequence, antibodies specific for each isoform have now been generated (Fig. 1). Antibodies specific for Tpm1p fail to stain *tpm1Δ* cells (Fig. 2 *D*), and antibodies specific to Tpm2p fail to stain *tpm2Δ* cells, thereby demonstrating their specificity for immunofluorescence.

In wild-type cells, Tpm2p was detectable along actin cables like Tpm1p (Fig. 2, compare *C* and *E*). Further, in large-budded wild-type cells, both Tpm1p and Tpm2p were present as a bar at the mother/bud junction (Fig. 2 *C*, *arrowhead*). In favorable views, the tropomyosin bar resolved as a ring, reminiscent of the bud neck F-actin ring (Chant and Pringle, 1995; Epp and Chant, 1997; Lippincott and Li, 1998), suggesting that tropomyosins in *S. cerevisiae* may play a role in cytokinesis, as has been shown for the tropomyosin encoded by *cdc8* of *Schizosaccharomyces pombe* (Balasubramanian et al., 1992).

Loss of Tpm1p results in viable cells with no detectable actin cables and partial loss of polarization of the actin cortical patches, cell wall deposition, and growth (Liu and Bretscher, 1989*b*). In *tpm1Δ* cells, Tpm2p was restricted to the vicinity of sites of active growth: nascent bud sites in

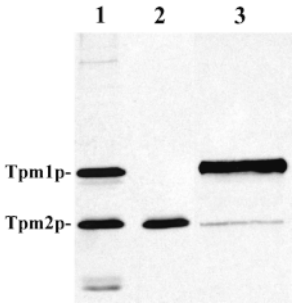

Figure 1. Specificity of affinity-purified antibodies used in these studies. Western blots of whole cell yeast extract using: lane *1*, B43 antiserum from which the Tpm2p-specific antibodies were isolated; lane *2*, Tpm2p-specific antibodies; and lane *3*, Tpm1p-specific antibodies.

unbudded cells, bud tips in small-budded cells, and a diffuse distribution in the buds of medium-budded cells (Fig. 2 *F*). Although this distribution overlapped the distribution of actin cortical patches, the two did not colocalize, suggesting Tpm2p is not incorporated into patches. Tpm2p did not appear in extended cables either, which is consistent with the finding that *tpm1Δ* cells lack detectable actin cables. Rather, the appearance of Tpm2p, particularly in small buds, resembled the staining seen for tropomyosin in the small buds of wild-type yeast (for comparison to Tpm1p see Fig. 2 *C*, *insets*). The overlapping distribution of cortical patches with Tpm2p in *tpm1Δ* cells prevented determination of whether there is F-actin specifically associated with Tpm2p in these cells. Tpm2p also appeared as a bar between the bud and mother cell in large-budded *tpm1Δ* cells (Fig. 2 *F*, *arrowhead*), again suggesting a role in cytokinesis.

The small Rab-GTPase, Sec4p, is an essential component of secretory vesicles involved in their polarized delivery (Goud et al., 1988; Walch-Solimena et al., 1997). The unconventional type V myosin, Myo2p, has also been suggested to be involved in the polarized delivery of secretory vesicles (Johnston et al., 1991; Govindan et al., 1995). The enrichment of both Myo2p and Sec4p near regions of cell growth in wild-type cells is consistent with these proposals (Fig. 2, *G* and *I*; Brennwald and Novick, 1993; Lillie and Brown, 1994). Since *tpm1Δ* cells are viable and able to bud, albeit with reduced polarity, the localization of Sec4p and Myo2p was examined in these cells; both showed a polarized distribution, similar to that found in wild-type cells (Fig. 2, *H* and *J*).

Isolation of tpm2Δ tpm1 Temperature-sensitive Mutants

To examine the short-term effects of the loss of all functional tropomyosin, we generated conditional *tpm1* mutations (*tpm1-1* and *tpm1-2*) in a *tpm2Δ* background (Fig. 3 *A*). Both *tpm1-1 tpm2Δ* cells and *tpm1-2 tpm2Δ* cells were found to grow at temperatures below 34°C, but were inviable at 34.5°C or greater. Both alleles could be suppressed by either *TPM1* or *TPM2*, as expected, but were unable to suppress each other. The alleles were also suppressed by expression of rat skeletal muscle tropomyosin (data not shown).

When cells expressing Tpm1p from either *tpm1-1* (ABY 950) or *tpm1-2* (ABY944) were shifted to restrictive temperatures for up to 4 h, the amount of tropomyosin present did not decrease relative to total protein (Fig. 3 *B*). Therefore, the proteins are not degraded at the restrictive temperature, but become nonfunctional.

Yeast Lacking Functional Tropomyosins Grow Isotropically and Have a Completely Depolarized Actin Cytoskeleton

When observed at permissive temperatures, the *tpm1-1* and *tpm1-2* alleles displayed different phenotypes. Cells bearing *tpm1-1 tpm2Δ* (ABY950) resembled *tpm1Δ TPM2* cells morphologically and in actin distribution, suggesting that the protein has only partial function at permissive temperatures. By contrast, *tpm1-2 tpm2Δ* (ABY944) cells were indistinguishable from wild-type cells in terms of growth rates and morphology and had actin cables, though fainter than those seen in wild-type cells (Fig. 4, *A*, *C*, and

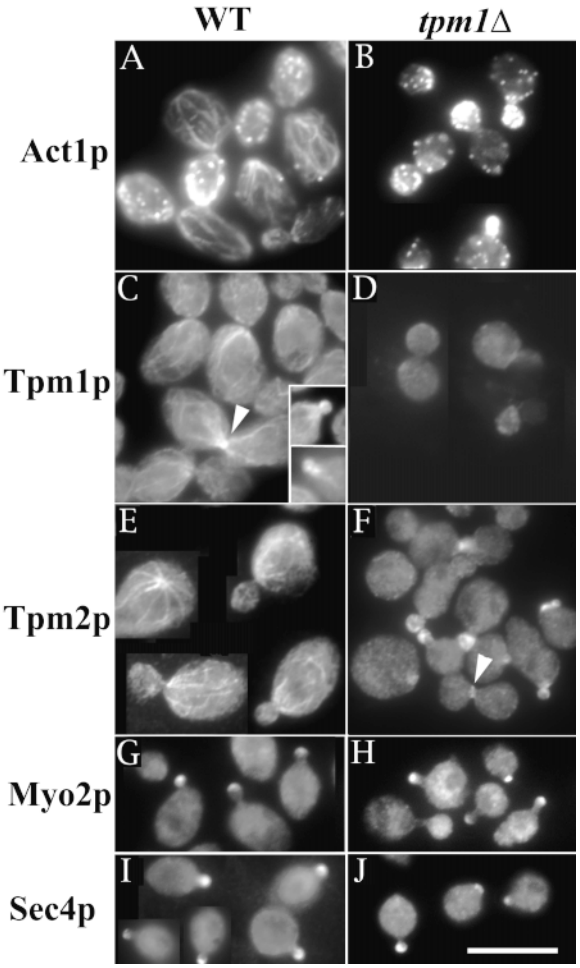

Figure 2. Cytoskeletal and secretory protein distributions in ABY913 wild-type (*A*, *C*, *E*, *G*, and *I*) and ABY161 *tpm1Δ/tpm1Δ* (*B*, *D*, *F*, *H*, and *J*) diploids. Selected cells are shown stained with antibodies for actin (*A* and *B*), Tpm1p (*C* and *D*), Tpm2p (*E* and *F*), Myo2p (*G* and *H*), and Sec4p (*I* and *J*). The insets in *C* display small buds for comparison to the Tpm2p staining in *F*. The arrowheads in *C* and *F* indicate Tpm1p- and Tpm2p-containing bars at the mother/bud neck that resemble reported cytokinetic F-actin rings. Images of actin immunofluorescence have been brightened to enhance the detection of actin cables at the expense of the resolution of actin cortical patches. Bar, 10 μm.

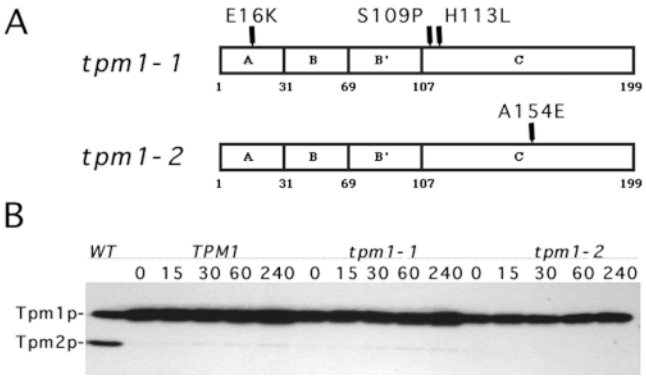

Figure 3. (*A*) Amino acid substitutions of *tpm1-1* and *tpm1-2*. Boxed regions A, B, B′, and C represent psuedorepeats common to tropomyosins (Drees et al., 1995). (*B*) Tpm1p from *tpm1-1* and *tpm1-2* is not degraded at 34.5°C. ABY945 *TPM1 tpm2Δ*, ABY950 *tpm1-1 tpm2Δ*, and ABY944 *tpm1-2 tpm2Δ* were incubated at 36°C for indicated times and whole cell yeast extracts were prepared and blotted with B43 (anti-Tpm1p/Tpm2p sera). The same amount of protein was loaded to each lane for each respective strain. *WT* is ABY913 *TPM1*/*TPM1 TPM2*/*TPM2*.

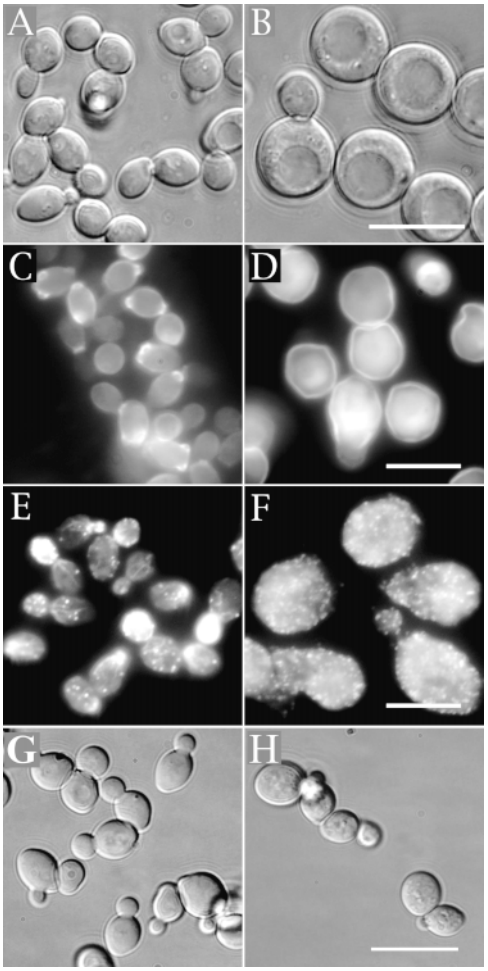

Figure 4. ABY971 *tpm1-2/tpm1-2 tpm2Δ/tpm2Δ* undergoes morphological changes when shifted from room temperature (*A*, *C*, and *E*) to 34.5°C for 4 h (*B*, *D*, and *F*), whereas secretion-defective ABY999 *sec6-4/sec6-4 tpm1-2/tpm1-2 tpm2Δ/tpm2Δ* does not (*G* and *H*). Cells were visualized by DIC microscopy (*A*, *B*, *G*, and *H*), stained with calcofluor to visualize chitin (*C* and *D*), or fixed and prepared for immunofluorescence with antiactin antibodies (*E* and *F*). Images of actin immunofluorescence have been brightened to enhance visibility of actin cables at the expense of the resolution of actin cortical patches. Bars, 10 μm.

E), indicating that the *tpm1-2* gene product is more fully functional at the permissive temperature. For this reason, all further work was carried out using *tpm1-2 tpm2Δ* cells.

The viability of *tpm1-2 tpm2Δ* cells was determined after shifting to the restrictive temperature of 34.5°C for varying lengths of time and then plating on rich medium at room temperature. For the first 2 h, the cells retained full viability, but then viability declined such that after 5 h at 34.5°C only 34% of cells plated were viable. This loss in viability is at least partially attributable to a time-dependent increase in the fraction of lysed cells observed microscopically.

When *tpm1-2 tpm2Δ* cells were shifted to the restrictive temperature of 34.5°C, growth continued but was completely depolarized. For small-budded cells, all growth occurred in the mother rather than in the bud, resulting after 4 h in huge round cells (Fig. 4 *B*). These large cells sometimes retained the small bud remnant, although in suspension the remnant often detached and floated away. Large-budded cells instead showed a thickening of the bud neck and also gradually grew into completely rounded cells. This depolarization of growth was much more complete than that seen in *tpm1Δ* cells, indicating that polarized growth is strictly dependent upon the presence of functional tropomyosin. Deposition of chitin was also completely depolarized. After 4 h, calcofluor stained uniformly over the entire cell surface with bud scars no longer visible (Fig. 4 *D*). This depolarized growth still depended upon an intact secretory pathway as *sec6-4 tpm1-2 tpm2Δ* cells showed no cell enlargement or morphological changes at restrictive temperatures (Fig. 4, *G* and *H*).

The actin cytoskeleton in *tpm1-2 tpm2Δ* cells completely depolarized after shifting to 34.5°C. When actin was examined, cables were no longer visible and the distribution of cortical patches became isotropic (Fig. 4 *F*). This demonstrates that tropomyosin is required for correct polarization of the actin cytoskeleton and that the remaining polarization seen in the *tpm1Δ TPM2* cells depends upon Tpm2p.

It has been shown that shifting wild-type cells to 37°C results in transient depolarization of the actin cytoskeleton (Lillie and Brown, 1994); both our wild-type and *tpm1-2 tpm2Δ* strains also lost cables and depolarized when shifted to 36°C, with wild-type cells recovering their polarity after ~20 min. However, 34.5°C, a restrictive temperature for *tpm1-2 tpm2Δ,* has little effect on the polarity of the actin cytoskeleton of our isogenic control strain (ABY973 *TPM1/TPM1 tpm2Δ/tpm2Δ*) (Fig. 5, *A–D*, and Fig. 6 *A*).

Whereas budding and polarized growth had ceased in *tpm1-2 tpm2Δ* cells at 34.5°C, mitosis still occurred. Staining of nuclei revealed a gradual increase in binucleate cells over a 5-h period. Before the temperature shift, no cells

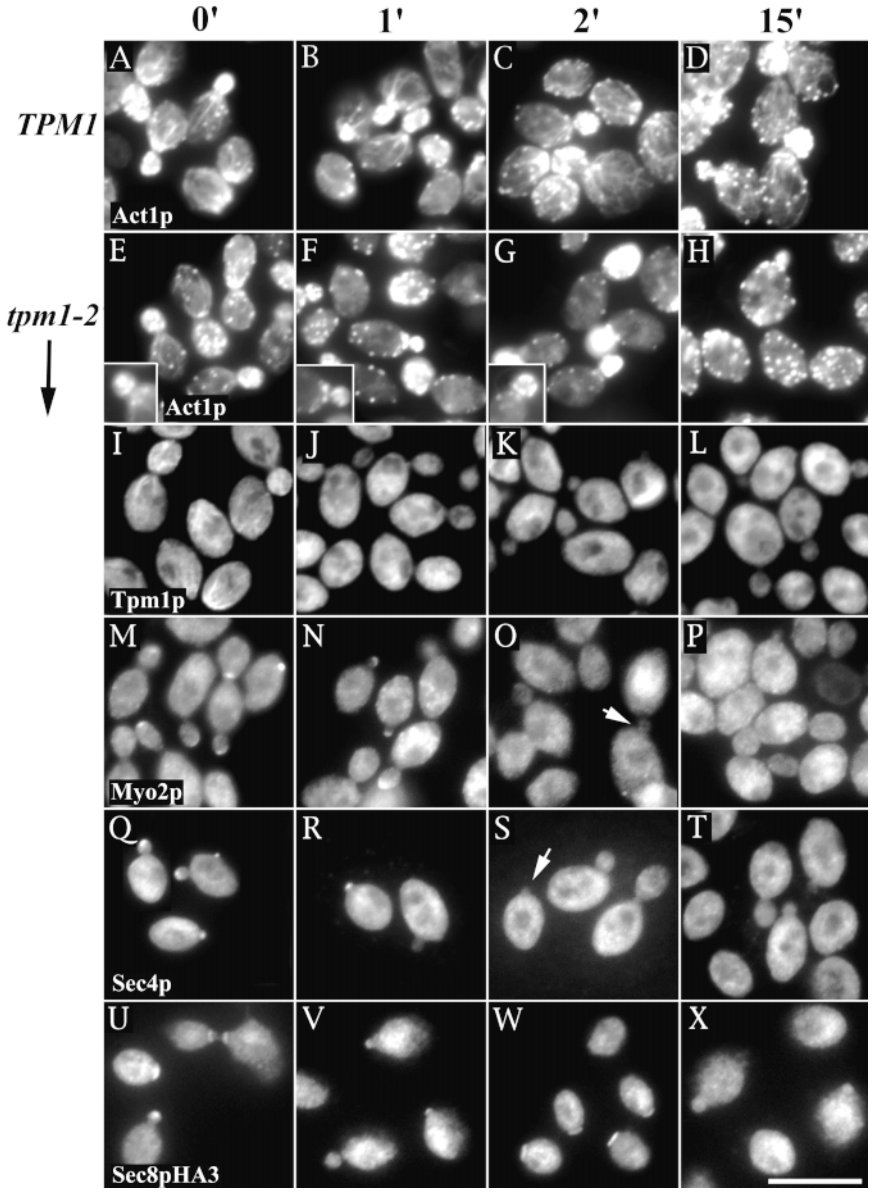

Figure 5. Shift to restrictive temperature rapidly disrupts cytoskeletal and secretory protein distributions in *tpm1-2 tpm2Δ* cells. ABY987 *TPM1*/*TPM1 tpm2Δ*/*tpm2Δ SEC8:HA3*/*SEC8:HA3* control (*A–D*) and ABY988 *tpm1-2*/*tpm1-2 tpm2Δ*/*tpm2Δ SEC8:HA3*/*SEC8:HA3* (*E–X*) were shifted to 34.5°C for 0 (*A*, *E*, *I*, *M*, *Q*, and *U*), 1 (*B*, *F*, *J*, *N*, *R*, and *V*), 2 (*C*, *G*, *K*, *O*, *S*, and *W*), or 15 min (*D*, *H*, *L*, *P*, *T*, and *X*) then fixed and prepared for immunofluorescence for actin (*A–H*), Tpm1p (*I–L*), Myo2p (*M–P*), Sec4p (*Q–T*), or HA epitope-tagged Sec8p (*U–X*). Arrows (*O* and *S*) indicate bud tips lacking Myo2p or Sec4p staining, respectively. Insets in *E–G* show actin cortical patch distribution within small buds. Other images of actin immunofluorescence have been brightened to enhance the detection of actin cables at the expense of the resolution of actin cortical patches. Bar, 10 μm.

contained >1 nucleus, while after 5 h at 34.5°C, 40% of unlysed cells were binucleate and 1% had >2 nuclei. However, the onset of mitosis was much slower than expected. While the doubling time for the isogenic *TPM1* strain is 1.5 h at 34.5°C, only 15% of *tpm1-2 tpm2Δ* cells had undergone nuclear division after 1.5 h, suggesting a cell cycle checkpoint had been activated to delay mitosis, perhaps the actin cytoskeleton-dependent checkpoint described previously (Lew and Reed, 1995; McMillan et al., 1998).

Loss of Cables in Tropomyosin Mutant Cells Is Extremely Rapid Whereas the Depolarization of Cortical Patches Is Gradual

Since after 4 h at 34.5°C *tpm1-2 tpm2Δ* cells lack both actin cables and cortical patch polarity, we examined the speed of these cytoskeletal changes by staining actin in cells fixed at earlier time points. Remarkably, actin cables were not detectable in these cells within 1 min after shifting to 34.5°C (Fig. 5, *E–H*, and Fig. 6 *B*), whereas *TPM1 tpm2Δ* control cells retained cables (Fig. 5, *A–H*, and Fig. 6 *A*). We worried that actin cables might still be present at 1 min but that fixation was too slow to preserve them against subsequent disassembly. To rule out this possibility, *tpm1-2 tpm2Δ* cells were subjected to various temperature shift and fixation protocols and stained for actin. Actin cables were seen when cells were fixed at room temperature for 1.5 h (Fig. 7 *A*), but not when cells were prewarmed for 1 min at 34.5°C before fixation at room temperature (Fig. 7 *B*). However, when cells were fixed for 10 s at room temperature and then shifted to 34.5°C for 1 min followed by 1.5 h at room temperature, cables were clearly evident (Fig. 7 *C*). Thus, 10 s of fixation is sufficient time to preserve cables through a shift to 34.5°C for 1 min. We con-

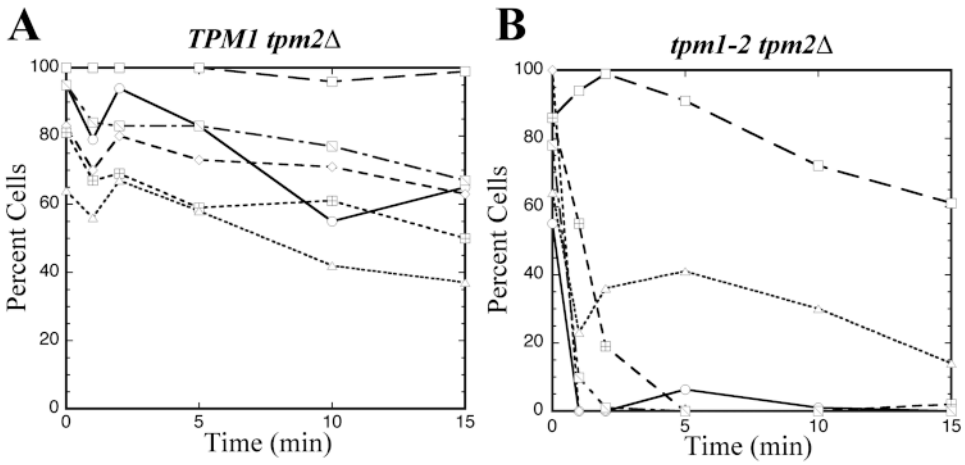

Figure 6. Shift to restrictive temperature rapidly disrupts cytoskeletal and secretory protein distributions in *tpm1-2 tpm2Δ* cells. ABY987 *TPM1/TPM1 tpm2Δ/tpm2Δ SEC8:HA3/SEC8:HA3* control (*A*) and ABY988 *tpm1-2/tpm1-2 tpm2Δ/tpm2Δ SEC8:HA3/SEC8:HA3* (*B*) were shifted to 34.5°C for 0, 1, 2, 5, 10, and 15 min. Small-budded cells, defined as having a bud diameter half of or less than the mother cell diameter, were scored for the presence of the following markers: actin cables ( ), cortical patches clustered in the bud ( ), Tpm1p-staining cables (*diamonds*), Myo2p cap ( ), Sec4p cap (*striped boxes*), and Sec8 pHA3 cap ( ). 100–300 cells were scored per data point.

clude that detectable actin cables disassemble in *tpm1-2 tpm2Δ* cells within 1 min of shifting to 34.5°C, demonstrating that the conditional phenotype appears very rapidly and that cables are highly unstable in the absence of functional tropomyosin.

Loss of tropomyosin localization was equally rapid (Fig. 5, *I–L*, and Fig. 6 *B*). Whereas tropomyosin-staining cables were evident in *tpm1-2 tpm2Δ* cells at permissive temperatures, Tpm1p staining was diffuse within 1 min of shifting to 34.5°C. *TPM1 tpm2Δ* control showed virtually no loss of cable staining through 15 min at 34.5°C (Fig. 6 *A*). We confirmed the rapidity of fixation of Tpm1p-staining cables using the same control as described for actin above. The Tpm1p-staining ring noted at the necks of large-budded cells also vanished within 1 min at 34.5°C. Thus, although the tropomyosin protein in *tpm1-2 tpm2Δ* cells is stable at the restrictive temperature (Fig. 3 *B*), it cannot stabilize actin cables or assemble at the bud neck at restrictive temperatures.

In contrast, the distribution of actin cortical patches remained polarized and unperturbed for the first 5 min after shifting to 34.5°C, and then gradually became depolarized over the next 10–20 min (Figs. 5 *H* and 6 *B*). For the first 5 min, clustering of cortical patches did not appear to be disturbed (sample small buds are depicted in Fig. 5, *E–G*, *insets*). Another cortical patch component, the unconventional type I myosin, Myo5p, was examined in *tpm1-2 tpm2Δ* cells by tagging the chromosomal *MYO5* locus with a triple-HA epitope; COOH-terminal tagging of this gene does not interfere with its function (Goodson et al., 1996). After shifting to 34.5°C, Myo5pHA3 remained colocalized with actin cortical patches throughout a 15-min time course (data not shown). Similarly, a GFP-tagged capping protein, GFPCap2p, which also has been shown to be functional and to colocalize with cortical patches (Waddle et al., 1996), gradually assumed a depolarized distribution in *tpm1-2 tpm2Δ* cells in a manner indistinguishable from that observed for actin. Thus, cortical patches appear to initially retain their polarized distribution after loss of tropomyosin function, but gradually depolarize in the absence of tropomyosin-containing cables.

Membrane Trafficking in Tropomyosin-deficient Yeast Still Occurs Efficiently

Fluid-phase endocytosis has been shown to depend upon an intact actin cytoskeleton, and to be abolished in cells lacking functional components of cortical patches, such as actin (Act1p), fimbrin (Sac6p), and cofilin (Cof1p) (reviewed in Geli and Riezman, 1998; Wendland et al., 1998). To determine whether fluid phase endocytosis still occurs in the absence of functional tropomyosin, *tpm1-2 tpm2Δ* cells were incubated at 36°C for 1 h, then Lucifer yellow was added as an endocytic tracer for another hour at 36°C. The tropomyosin double mutant accumulated the dye to the same extent as wild-type control cells (data not shown).

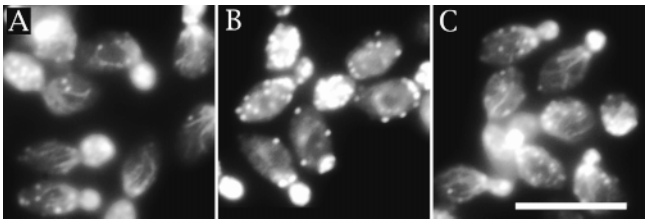

Figure 7. Formaldehyde fixation preserves actin cables rapidly. ABY971 *tpm1-2/tpm1-2 tpm2Δ/tpm2Δ* was grown at room temperature and treated for actin immunofluorescence after: (*A*) fixation for 1.5 h at room temperature; (*B*) shift to 34.5°C for 1 min, followed by addition of fixative, then incubation for a further 1.5 h at room temperature; and (*C*) addition of fixative and incubation at room temperature for 10 s, shift to 34.5°C for 1 min, then continued incubation for 1.5 h at room temperature. Images of actin immunofluorescence have been brightened to enhance the detection of actin cables at the expense of the resolution of actin cortical patches. Bar, 10 μm.

Post-Golgi trafficking of secretory vesicles has also been shown to be affected in cells conditionally defective in actin function (Novick and Botstein, 1985). Recently, it has been found that two secretory markers, invertase and the cell wall endoglucanase encoded by *BGL2*, are transported from the Golgi apparatus to the plasma membrane by separate vesicle populations (Harsay and Bretscher, 1995). Therefore, we examined whether either of these markers accumulated in *tpm1-2 tpm2Δ* cells at their restrictive temperature. After induction of invertase at 36°C for 1 h, cells were fractionated into external (cell wall and periplasmic) and internal protein and assayed for invertase activity. For both the *tpm1-2 tpm2Δ* mutant and *TPM1 tpm2Δ* control, all glycosylated invertase produced was efficiently exported, while a secretion-defective control strain (*sec6-4*) retained all glycosylated invertase internally (data not shown). To examine whether Bgl2p accumulated internally, *tpm1-2 tpm2Δ* and *TPM1 tpm2Δ* cells were incubated at 36°C for 1, 2, 3, or 4 h, fractionated into external and internal fractions, and assayed for Bgl2p by Western blot. The distribution of internal versus external protein was identical between the *TPM1 tpm2Δ* control and *tpm1-2 tpm2Δ* cells (data not shown).

Since vesicles resembling post-Golgi secretory vesicles accumulate in a fraction of *tpm1Δ TPM2* cells (Liu and Bretscher, 1992), we examined *tpm1-2 tpm2Δ* cells by thin section electron microscopy for accumulation of secretory membranes. *TPM1 tpm2Δ*, *tpm1-2 tpm2Δ*, and *sec6-4* strains were shifted to 36°C for 20 min, fixed, and processed for electron microscopy. A subset of *tpm1-2 tpm2Δ* cell profiles showed an accumulation of membrane-bound structures in their cytoplasm identical to those accumulated in the *sec6-4* strain at 36°C (Fig. 8 *A*, compare arrows in panel *b* to panels *c* and *d*). However, only 15% of the *tpm1-2 tpm2Δ* cells showed such structures, which was much less than the *sec6-4* control (85%). Further, the accumulation was not temperature dependent (Fig. 8 *B*). Therefore, both bulk secretion and fluid phase endocytosis occur efficiently in the absence of functional tropomyosin.

Loss of Tropomyosin and Cables Leads to a Rapid Delocalization of Myo2p and Sec4p and a Much Slower Delocalization of Sec8p

Since membrane trafficking remains efficient in the absence of functional tropomyosin, we wished to determine whether spatial targeting of secretion was affected by tropomyosin defects. As previously discussed, Myo2p and Sec4p distributions correlate with directed growth. The localization of Myo2p and Sec4p was examined after shifting *tpm1-2 tpm2Δ* cells to 34.5°C.

Myo2p became delocalized rapidly, appearing as a diffuse stain after 2 min (Fig. 5, *M–P*, and Fig. 6 *B*), whereas in control cells (*TPM1 tpm2Δ*) the distribution of Myo2p did not change (Fig. 6 *A*). Sec4p also rapidly delocalized in *tpm1-2 tpm2Δ* cells at 34.5°C (Fig. 5, *Q–T*, and Fig. 6 *B*). Again, *TPM1 tpm2Δ* control cells were not perturbed significantly (Fig. 6 *A*).

The effect on the polarized distribution of Sec8p was also examined. Sec8p is a component of the exocyst, a complex of eight proteins necessary for the fusion of secretory vesicles to the plasma membrane (Novick et al., 1980; TerBush et al., 1996). This complex also colocalizes with regions of cell growth (TerBush and Novick, 1995). Sec8p was examined in *tpm1-2 tpm2Δ* cells by replacing the endogenous *SEC8* locus with COOH-terminally HA epitope–tagged *SEC8*. Since this is the sole copy of the essential *SEC8* and replacement conferred no deleterious phenotype, *SEC8:HA3* must provide functional Sec8p. Immunofluorescence microscopy revealed that shifting *tpm1-2 tpm2Δ* cells to 34.5°C initially had no effect on the localization of Sec8pHA3. With longer incubations, the polarized staining decreased significantly, although some bud tip enrichment of Sec8pHA3 was evident in *tpm1-2 tpm2Δ* cells even after 15 min at 34.5°C (Fig. 5, *U–X*, and Fig. 6 *B*), indicating Sec8p is able to remain localized independent of actin cables. Prolonged incubation at 34.5°C (1 h) eventually delocalized Sec8pHA3. Conversely, although *TPM1* cells had a modest decrease in Sec8pHA3 polarization at 34.5°C over a 15-min time course (Fig. 6 *A*), by 1 h they had reestablished a strong polarized distribution of Sec8 pHA3.

Cables Quickly Reassemble in Tropomyosin Mutants with Rapid Repolarization of Myo2p, Sec4p, and Sec8p

To examine the effects of the restoration of functional tropomyosin, we studied recovery of the tropomyosin double mutant from the restrictive temperature. *tpm1-2 tpm2Δ* cells were incubated at 34.5°C for 1 h to completely depolarize the actin cytoskeleton, then cooled to 26°C for various times before fixation and localization of actin and Tpm1p. Astonishingly, *tpm1-2 tpm2Δ* cells showed restoration of Tpm1p-containing cables within 1 min, changing from a diffuse Tpm1p staining to a filamentous one (Fig. 9 *A*, *a* and *b*). In ~37% of cells examined after just 1 min of recovery, cables visibly emanated from a single focus within the cell (Fig. 9 *A*, *arrowheads* in *a*, and Fig. 10). Actin-staining cables were not readily apparent (using actin antibodies) in most cells at early recovery times (for example, Fig. 9 *C*, *m–o*). However, we assume tropomyosin is associating with F-actin for several reasons. First, tropomyosin is only known to assemble into filaments under physiological conditions in the presence of F-actin. Second, double-labeling of recovering cells for Tpm1p and actin (by rhodamine-phalloidin staining) showed colocalization of Tpm1p with a focal point of actin (Fig. 9 *D*, *q* and *r*). Third, although the conditions used for double-labeling using rhodamine-phalloidin were not optimal for preserving nascent cables, when Tpm1p-positive cables were noted under those conditions, they also stained with rhodamine-phalloidin (Fig. 9 *D*, *q* and *r*). We attribute the lack of cable staining with actin antibodies to high background fluorescence from abundant cortical patches.

Myo2p, Sec4p, and Sec8pHA3 rapidly repolarized at 26°C (Fig. 9 *A*, *c–h*, and Fig. 10), although recovery of Sec8pHA3 appeared delayed by ~1 min relative to Sec4p and Myo2p (Fig. 10, *arrowhead*). Double-labeling for Myo2p and Sec4p (Fig. 9 *D*, *u* and *v*) and for Myo2p and Sec8pHA3 (Fig. 9 *D*, *w* and *x*) showed these proteins all polarized to the same location in recovering cells. Further, double-labeling for Tpm1p and Myo2p (data not shown) and for Tpm1p and Sec4p (Fig. 9 *D*, *s* and *t*) showed that

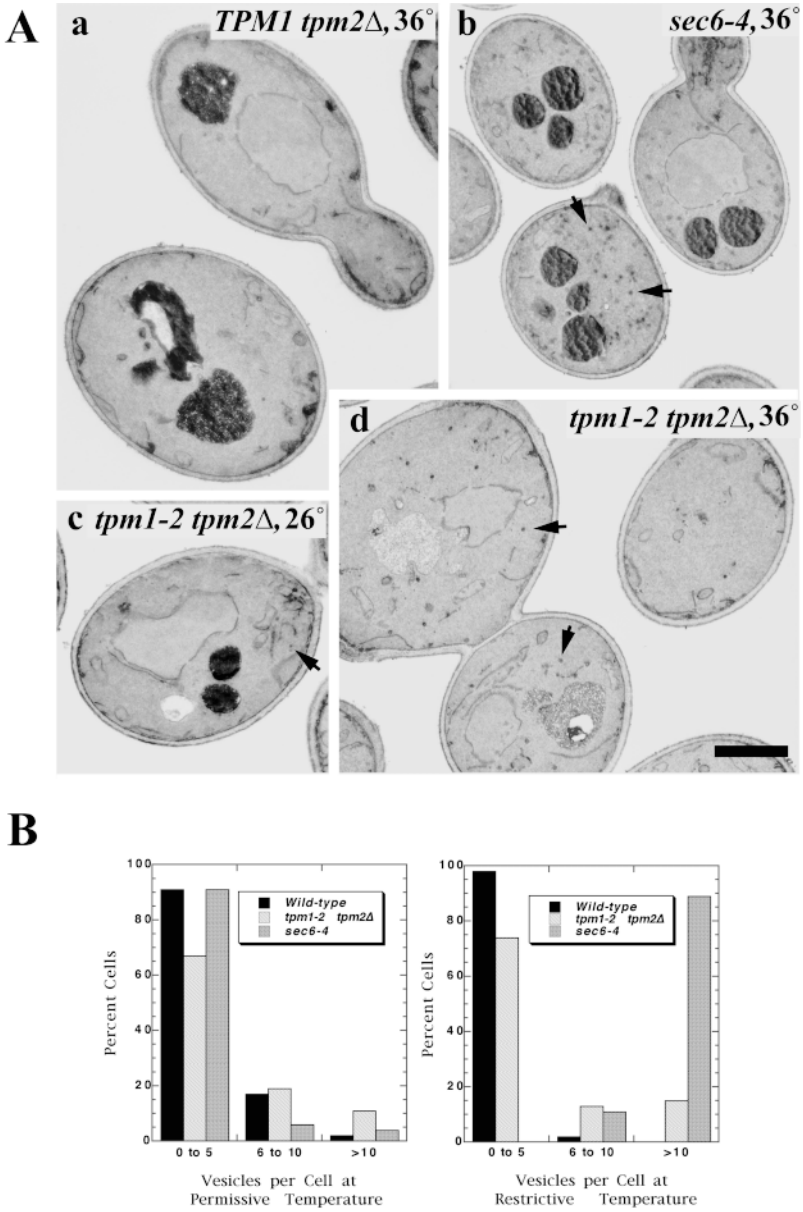

Figure 8. Vesicle accumulation after shift to restrictive temperature. (*A*) ABY973 *TPM1/TPM1 tpm2Δ/tpm2Δ* (*a*), ABY971 *tpm1-2/tpm1-2 tpm2Δ/tpm2Δ* (*c* and *d*), and ABY703 *sec6-4* (*b*) were shifted to 36°C for 0 or 20 min, and fixed and prepared for thin section electron microscopy. Arrows in *b, c,* and *d* indicate vesicles. *d* shows examples of *tpm1-2 tpm2Δ* cells with several vesicles (the cells on the left) and few vesicles (the cell on the right). Bar, 1 μm. (*B*) ABY973, ABY971, and ABY703 were scored for the accumulation of vesicular profiles. 52–55 cells were scored per data point.

Myo2p and Sec4p both repolarized at the convergence of the tropomyosin-containing cables. The recovery of these markers was even faster when the recovery temperature was 11°C, with significant polarization of cables (40% cells viewed) and Myo2p visible in as little as 10 s, showing that both cable reformation and cable-dependent transport are extremely rapid.

With repolarization of the secretory pathway, budding resumed in *tpm1-2 tpm2Δ* cells. Tropomyosin double mutant cells were placed under 2% agarose/synthetic medium and incubated for 4 h at 35°C, resulting in large, round unbudded cells (Fig. 9 *B*, *i*). The cells were then cooled to 26°C over a 5-min period and permitted to recover. Bud emergence resumed rapidly, in that within 5 min of reaching 26°C, new growing buds were visible (Fig. 9 *B*, *j–l*). The recovering cells did not resume budding in a uniform manner. While some established new buds quickly, others delayed formation of a new bud for 1 h or more. This correlates with the observation that not all cells showed a rapid repolarization of Tpm1p, Myo2p, Sec4p, or Sec8p during recovery (Fig. 10).

The overall distribution of cortical patches did not change during the short time points at 26°C during which Myo2p, Sec4p, and Sec8p repolarized (Fig. 9 *C*, *m–o*). Rather, between 15 and 30 min were required for patches to resume an overall polarized distribution (Fig. 9 *C*, *arrows* in *p* show cells with repolarized cortical patches). Observation of Myo5pHA3 and Cap2pGFP yielded identical results, suggesting that cortical patches repolarize slowly with the restoration of actin cables. However, double-labeling of actin with Tpm1p (Fig. 9 *D*, *q* and *r*) and with Myo2p (data not shown) showed a localized concentration

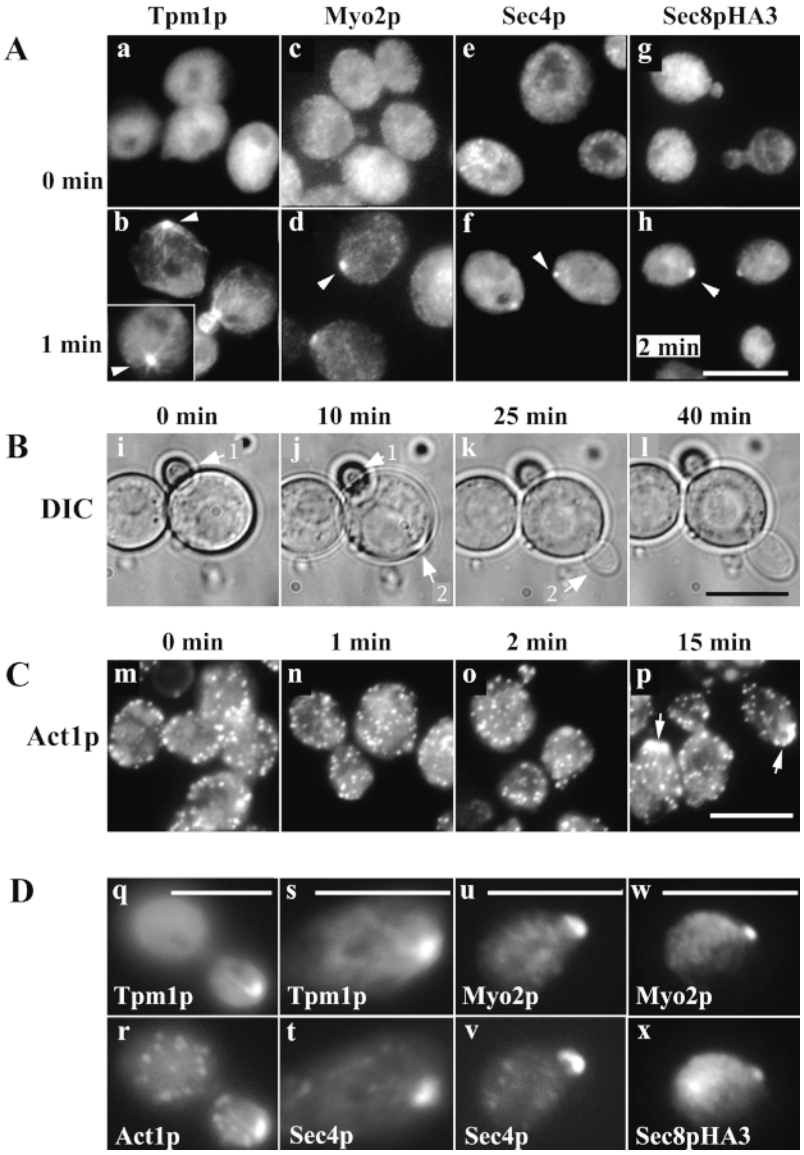

Figure 9. Recovery of ABY988 *tpm1-2/tpm1-2 tpm2Δ/tpm2Δ SEC8:HA3/SEC8:HA3* at room temperature after incubation at restrictive temperature. (*A*) Several cytoskeletal and secretory proteins repolarize rapidly: ABY988 was incubated at 34.5°C for 1 h then cooled to 26°C for either 0 (*a*, *c*, *e*, and *g*), 1 (*b*, *d*, and *f*), or 2 min (*h*) before fixation. Fixed cells were processed for immunofluorescence to detect Tpm1p (*a* and *b*), Myo2p (*c* and *d*), Sec4p (*e* and *f*), or epitope-tagged Sec8p (*g* and *h*). Arrowheads indicate repolarized protein. (*B*) Budding resumes quickly at the permissive temperature: ABY988 was incubated at 35°C for 4 h, then cooled to 26°C. DIC images of growing cells were acquired 0, 10, 25, and 40 min after cooling (*i–l*). The arrow (*1*) designates a bud grown before the shift to 35°C, then abandoned during growth at 35°C. The arrow (*2*) designates a newly emerging bud. (*C*) Repolarization of actin cortical patches is more gradual: ABY988 was incubated at 34.5°C for 1 h then cooled to 26°C for 0 (*m*), 1 (*n*), 2 (*o*), or 15 min (*p*) before fixation. Fixed cells were treated for immunofluorescence using Act1p-specific antibodies. Arrows in *p* denote cells showing cortical patch polarity and visible actin cables. (*D*) Double-labeling of repolarized cytoskeletal and secretory proteins: ABY988 was incubated at 34.5°C for 1 h, cooled to 26°C for 2 min, then fixed. Cells were double labeled for: Tpm1p and actin (rhodamine-phalloidin staining) (*q* and *r*); Tpm1p and Sec4p (*s* and *t*); Myo2p and Sec4p (*u* and *v*); Myo2p and epitope-tagged Sec8p (*w* and *x*). Bars, 10 μm.

of actin at the focal points for those two proteins at early recovery times, but we have not determined whether that actin corresponds to locally clustered cortical patches.

Repolarization of Sec4p and Sec8p Requires Myo2p

To determine whether the rapid recovery of Sec4p and Sec8p depends upon Myo2p, those markers were examined in a *myo2-66 tpm1-2 tpm2Δ SEC8:HA3* strain. At the permissive temperature, Myo2p, Sec4p, and Sec8p all showed a wild-type distribution, and after 1 h at 34.5°C they all stained diffusely. When permitted to recover at 26°C for 5 min, however, only a small percentage of the cells showed any recovery of Myo2p to a single focal point, in contrast to the 77% recovery seen in the *MYO2 tpm1-2 tpm2Δ SEC8:HA3* control (Fig. 11). This demonstrates that in the *myo2-66* mutant, Myo2p remains nonfunctional for longer than 5 min after returning to the permissive temperature. Under these conditions, polarized cables detected with Tpm1p antibodies reformed in the *myo2-66 tpm1-2 tpm2Δ* cells to the same extent as in the *MYO2* control. After 5 min of recovery, *myo2-66 tpm1-2 tpm2Δ* cells also showed very little repolarization of either Sec4p or Sec8pHA3 (Fig. 11). Therefore, polarized actin cables can reform despite reduced Myo2p function, but Sec4p and Sec8pHA3 do not repolarize without functional Myo2p.

Discussion

This study establishes that actin cables in budding yeast target the delivery of secretory vesicles by Myo2p, and thus direct the polarity of bud growth. We have isolated yeast with conditionally defective tropomyosin, and demonstrated that several proteins involved in polarizing secretion respond very rapidly to the presence of functional tropomyosin and actin cables, but are unaffected by the overall distribution of cortical actin patches.

Tropomyosin is essential to budding yeast, since deletion of both tropomyosin genes, *TPM1* and *TPM2*, is le-

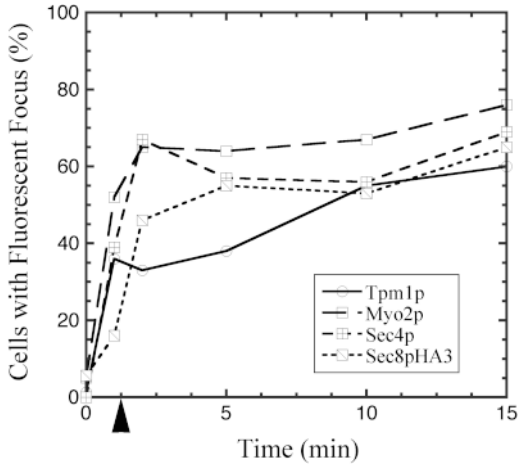

Figure 10. Repolarization of cytoskeletal and secretory proteins. ABY988 *tpm1-2/tpm1-2 tpm2Δ/tpm2Δ SEC8:HA3/SEC8:HA3* was incubated at 34.5°C for 1 h then shifted back to 26°C for recovery and fixed after 0, 1, 2, 5, 10, or 15 min. Cells were then treated for immunofluorescence to visualize Tpm1p(—), Myo2p(—), Sec4p(···), or HA epitope-tagged Sec8p(···). Cells were quantitated for the presence or absence of a visible focal point of fluorescence. 100–300 cells per data point were scored. Arrowhead indicates a 1-min time point where recovery of Sec8pHA3 lags behind the other markers.

thal (Drees et al., 1995). A recent report has suggested that tropomyosin may not be essential (Kagami et al., 1997); however, further analysis of strains thought to lack tropomyosin revealed that they still express Tpm2p. Additional experiments have confirmed that the loss of all tropomyosin is indeed lethal (our results and Kagami, M., A. Toh-e, and Y. Matsui, personal communication).

Actin cables require functional tropomyosin for stability. In wild-type cells, both Tpm1p and Tpm2p localize specifically to actin cables and, in large-budded cells, to a bud neck ring, but they are not associated with actin cortical patches. Although *tpm1Δ* cells lack detectable actin cables, Tpm2p is still localized to regions of cell growth and actin concentration. Furthermore, although Tpm2p staining in these cells overlaps cortical patches, it does not colocalize with patches. Rather, Tpm2p staining, particularly in small-budded *tpm1Δ* cells, resembles the appearance of tropomyosin in the small buds of wild-type cells, suggesting it may be associated with truncated cable-like structures within the bud. Since overexpression of Tpm2p in *tpm1Δ* cells produces extended actin cables, the absence of detectable cables may simply reflect the lower overall level of tropomyosin in *tpm1Δ* cells, which is about eightfold less than in wild-type cells (Drees et al., 1995). As Tpm2p binds avidly to F-actin (Drees et al., 1995), we suggest that Tpm2p in these cells is bound to truncated actin cables in the bud and possibly longer tenuous cables in the mother, too thin for detection by light microscopy. Work by Karpova et al. (1998) showing that actin cables can vary in thickness along their length supports this possibility. The presence of tenuous tropomyosin-containing actin cables in *tpm1Δ* cells would explain how Sec4p and Myo2p become polarized despite the absence of detectable actin cables in the mother cell.

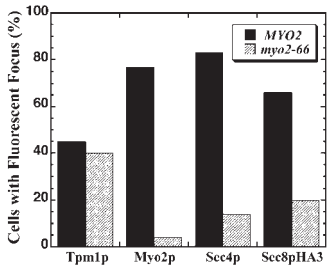

Figure 11. Myo2p is required for restoration of polarity of secretory proteins. ABY988 *tpm1-2/tpm1-2 tpm2Δ/tpm2Δ SEC8:HA3/SEC8:HA3* and ABY1100 *myo2-66 tpm1-2 tpm2Δ SEC8:HA3* were incubated at 34.5°C for 1 h, then permitted to recover at 26°C for 5 min, fixed, and treated for immunofluorescence to visualize Tpm1p, Myo2p, Sec4p, or HA epitope–tagged Sec8p. Cells were then quantitated for the presence or absence of a visible focal point of fluorescence. 100–150 cells per data point were scored.

To study the short-term effects of the loss of tropomyosin, we generated a conditionally defective tropomyosin mutant. Specifically, we isolated a temperature-sensitive *tpm1-2* allele in a *tpm2Δ* background. Shifting the *tpm1-2 tpm2Δ* cells to 34.5°C results in the loss of tropomyosin function. A summary of the relationships between the presence of tropomyosin-containing actin cables and the polarity of several cell components is shown in Fig. 12.

The most rapid phenotype of the loss of functional tropomyosin is the disappearance of actin cables. Like wild-type tropomyosin, Tpm1p in *tpm1-2 tpm2Δ* cells localizes to actin cables as well as to a bud neck ring at permissive temperatures. However, within 1 min of shifting *tpm1-2 tpm2Δ* cells to 34.5°C, tropomyosin staining becomes diffuse, suggesting a rapid dissociation of the protein from F-actin structures (Fig. 12, step *1*). At the same time, actin cables vanish, possibly reflecting either depolymerization of their actin or unbundling of the actin filaments to the point that they can no longer be resolved. In support of the actin depolymerization model, study of the actin-depolymerizing drug latrunculin-A shows that the F-actin of cables is capable of rapid turnover (Ayscough et al., 1997). Further, a recent report by Belmont and Drubin (1998) suggests that loss of tropomyosin from cables can lead to recruitment of the actin-depolymerizing protein cofilin (Cof1p), and that the F-actin of tropomyosin-free cables would be depolymerized.

The product of *tpm1-2* is not degraded at high temperatures and the temperature-sensitive phenotype is rapidly reversible. When *tpm1-2 tpm2Δ* cells are restored to a permissive temperature, cables reappear within 1 min, suggesting that cables are highly dynamic structures that can assemble quickly (Fig. 12, step *5*). Reassembled cables converge upon a single point, demonstrating that their polarity is reestablished as they reform. Again, two models of reassembly are possible. If cable disassembly reflected actin depolymerization, cable reformation would reflect a rapid polymerization event. If cable disassembly were due to unbundling, cable reformation may reflect rapid binding of tropomyosin to preexisting fibers and the recruitment of an actin bundling protein to the tropomyosin/actin, leading to consolidation into cables.

Loss of tropomyosin and detectable actin cables leads to the loss of polarized growth. That is, when small-budded *tpm1-2 tpm2Δ* cells are shifted to 34.5°C, bud growth

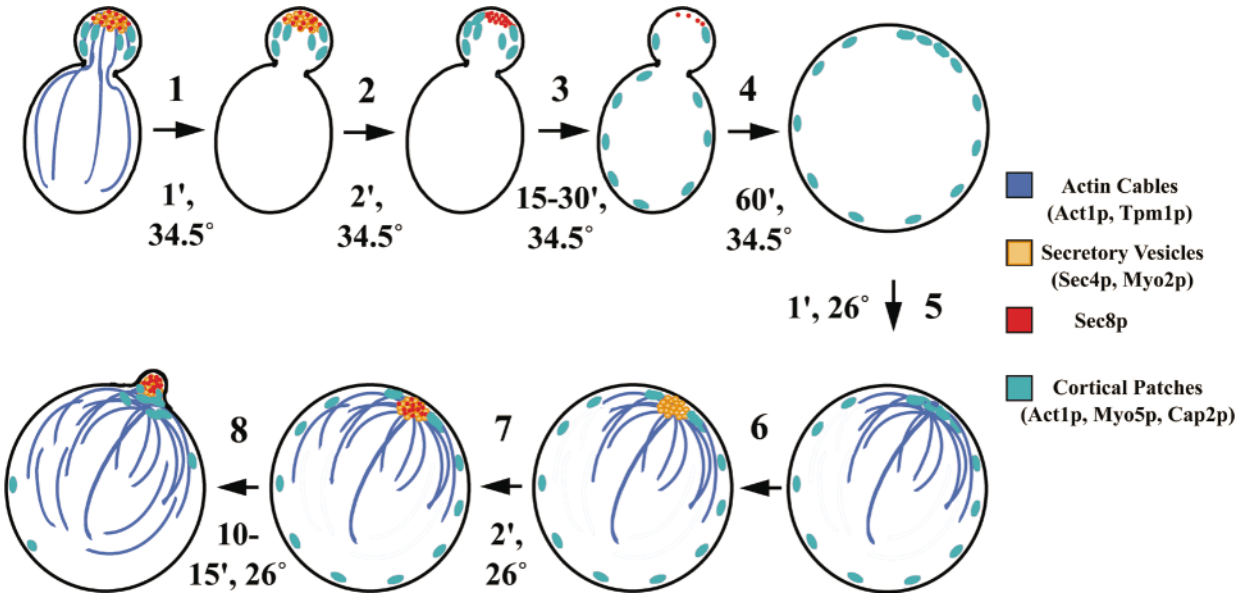

Figure 12. Steps of depolarization and repolarization in response to loss and gain of tropomyosin-containing cables in *tpm1-2 tpm2Δ* cells. Upon shift to 34.5°C, (*1*) 1 min: actin cables disappear, (*2*) 2 min: Myo2p and Sec4p staining at the bud tips is lost, (*3*) 15–30 min: cortical patches gradually assume an isotropic distribution and Sec8p staining at the bud tip diminishes, (*4*) 1 h: Sec8p completely delocalizes and isotropic growth occurs. Upon return to 26°C, (*5*) 1 min: actin cables reassemble, although this occurs as a distinct step only in *myo2-66* cells, (*6*) 1 min: Myo2p and Sec4p repolarize in *MYO2* cells as cables are reformed, (*7*) 2 min: Sec8p repolarizes, (*8*) 10–15 min: cortical patches are cleared from the mother and repolarize to the growing bud site.

ceases and the mothers become big and uniformly round. For large-budded cells, the tropomyosin neck ring disassembles and the bud neck thickens until distinction between the mother and daughter is lost, again generating uniformly round large cells. When tropomyosin function is restored, polarized growth resumes very rapidly.

This isotropic growth in *tpm1-2 tpm2Δ* cells reflects the loss of targeted secretion. An extremely tight correlation was seen between the presence of polarized cables and the polarized distribution of several proteins involved in targeted secretion, namely: the secretory vesicle-bound Rab-GTPase Sec4p, the unconventional type V myosin Myo2p, and the exocyst component Sec8p. Both Myo2p and Sec4p have been implicated in targeting secretory vesicles (Johnston et al., 1991; Govindan et al., 1995; Walch-Solimena et al., 1997). All three proteins are localized to regions of cell growth, paralleling the polarization of both actin cables and actin cortical patches (Adams and Pringle, 1984; Brennwald and Novick, 1993; Lillie and Brown, 1994; TerBush and Novick, 1995), although it had not been clear how they might interact with the actin cytoskeleton.

When tropomyosin-containing actin cables are lost from *tpm1-2 tpm2Δ* cells, Myo2p and Sec4p become delocalized within 2 min (Fig. 12, step *2*). When cables are restored, Sec4p and Myo2p repolarize within minutes (Fig. 12, step *6*), demonstrating a rapid response of those two proteins to the presence of tropomyosin-bound actin cables and indicating that the newly restored cables are functional for transport of secretory components. The swift recruitment of Myo2p in response to actin cables suggests that the protein acts as a motor to translocate along actin cables to regions of cell growth and that the actin cables are polarized with their barbed ends directed toward regions of cell growth. The repolarization of Sec4p in response to newly formed actin cables depends upon Myo2p, as when recovery is observed in a *myo2-66 tpm1-2 tpm2Δ* triple mutant, Sec4p does not repolarize despite the formation of cables. This result agrees well with a previous report that Sec4p localization is Myo2p dependent (Walch-Solimena et al., 1997) and is consistent with models whereby Myo2p binds secretory vesicles (with attached Sec4p) and ferries them along actin cables to sites of cell growth.

Sec8p redistributes more gradually than Myo2p or Sec4p after the loss of tropomyosin function, suggesting it binds to the plasma membrane at sites of cell growth by an actin cable–independent method (Fig. 12, steps *3* and *4*). However, after extended periods in the absence of tropomyosin function, Sec8p also becomes delocalized, and, after the restoration of functional tropomyosin, Sec8p repolarizes very rapidly, though just delayed relative to Sec4p and Myo2p (Fig. 12, step *7*). The delay may reflect a need for some factor delivered by cables, probably secretory vesicles, to growth sites for Sec8p recruitment, but, once Sec8p is bound there, it can remain for longer periods in the absence of both actin cables and nascent secretory vesicles. Consistent with this view is the report that Sec8p depends upon secretion in order to remain localized (Finger et al., 1998). As further support, Sec8p repolarization, like Sec4p, depends upon functional Myo2p and does not occur in the *myo2-66 tpm1-2 tpm2Δ* mutant.

Cortical actin patch distribution was also perturbed by the loss of tropomyosin function, but the response, to any degree that we could detect, was more than 10 times slower than that of any of the above markers (Fig. 12, step *3*).

While either Tpm1p or Tpm2p alone can maintain at least a partially polarized distribution of cortical patches, with the total loss of functional tropomyosin, cortical patches migrated to an isotropic distribution over the cell surface. The composition of the cortical patches under these circumstances appeared normal in that two known patch components, Cap2p and Myo5p, remained associated with the patches. Upon restoration of actin cables, the cortical patches gradually repolarized (Fig. 12, step *8*), suggesting that the overall distribution of cortical patches depends somehow upon actin cables, possibly responding to some polarity cue delivered by cables to sites of growth. An overall polarized distribution of cortical patches is restored only after 10–15 min, although localized clustering of patches near the cable focal points occurs earlier.

Actin cortical patches are commonly thought to be the nucleators of actin cables. However, a recent report demonstrates that cables do not always terminate upon cortical patches (Karpova et al., 1998). Further, the report shows that actin cables can exist with cortical patches close to both ends, suggesting that association with patches is not an indicator of the inherent polarity of actin cables. Interestingly, Tpm1p-containing cables, Myo2p, Sec4p, and Sec8p all repolarize long before actin cortical patches resume an overall polarized distribution, suggesting cortical patches by themselves are not nucleators of actin cables. One possible explanation for this observation is that somehow a subset of cortical patches becomes established as nucleators of actin cables. An alternative explanation is that actin cables do not nucleate from cortical patches, but from some other site on the plasma membrane. It has been noted previously that Myo2p, Sec4p, and Sec8p all polarize similarly to cortical patches, but they do not colocalize with the patches (Brennwald and Novick, 1993; Lillie and Brown, 1994; Finger et al., 1998). The distribution of Myo2p, Sec4p, and Sec8p in wild-type cells might reflect their accumulation at a nucleation site where the barbed ends of actin cables converge that is distinct from cortical patches, explaining the lack of colocalization.

If cortical patches might not play a role in targeting secretion, what role might they play at regions of cell growth? One possibility is that cortical patches mediate some activity required to maintain efficient active growth. Actin patches are likely to function directly in endocytosis. There is a remarkable correlation between defects in components of cortical patches, such as Act1p/End7p, Arp2p, Cof1p, Sac6p, Dim2p/Pan1p, and Myo5p, and defects in endocytosis (reviewed in Geli and Riezman, 1998; Wendland et al., 1998). To maintain efficient secretion at the ends of cables throughout the cell cycle, actin cortical patches may be required to recycle membranes from those same locations to retrieve such components as v-SNARES and lipids for further rounds of exocytosis.

An interesting question is the nature of the polarizing signal that remains localized in *tpm1-2 tpm2Δ* cells to redirect actin cable assembly. Currently, the molecular nature of this polarizing cue is unknown. However, several proteins important to the establishment and maintenance of cell polarity and actin organization have been localized to the same regions toward which cables converge, notably the Rho-GTPases Cdc42p and Rho1p, as well as several proteins shown to interact with these GTPases, including the F-actin–binding protein Bem1p and the yeast formin Bni1p. Interestingly, Bni1p has been reported to bind two more actin-binding proteins, Bud6p/Aip3p and EF1α, as well as to yeast profilin, which could serve to locally stimulate F-actin formation and thereby nucleate cable reformation (reviewed in Tanaka and Takai, 1998). Further studies will be needed to determine which molecules remain polarized within cells lacking tropomyosin function. The use of appropriate mutants may then reveal which genes are required to generate polarized actin cables, and thereby establish polarity in budding yeast.

We are greatly indebted to Peter Novick (Yale University School of Medicine) for providing and Ruth Collins (Yale University School of Medicine) for transporting a generous supply of antibody to Sec4p, without which this study would not have been possible. We are also grateful to John Cooper (Washington University School of Medicine) for his donation of the *GFP:CAP2* construct, pBJ646.

This work was supported by National Institutes of Health grant GM39066.

Received for publication 9 September 1998 and in revised form 19 November 1998.

References

Adams, A., and J. Pringle. 1984. Relationship of actin and tubulin distribution to bud-growth in wild-type and morphogenetic-mutant *Saccharomyces cerevisiae. J. Cell Biol.* 98:934–945.

Adams, A., D. Johnston, R. Longnecker, B. Sloat, and J. Pringle. 1990. *CDC42* and *CDC43*, two additional genes involved in budding and the establishment of cell polarity in the yeast *Saccharomyces cerevisiae. J. Cell Biol.* 111:131–142.

Adams, A., D. Botstein, and D. Drubin. 1991. Requirement of yeast fimbrin for actin organization and morphogenesis *in vivo*. *Nature.* 354:404–408.

Amatruda, J., J. Cannon, K. Tatchell, C. Hug, and J. Cooper. 1990. Disruption of the actin cytoskeleton in yeast capping protein mutants. *Nature*. 344:352–354.

Amatruda, J., D. Gattermeir, T. Karpova, and J. Cooper. 1992. Effects of null mutations and overexpression of capping protein on morphogenesis, actin distribution, and polarized secretion in yeast. *J. Cell Biol.* 119:1151–1162.

Ayscough, K., J. Stryker, N. Pokala, M. Sanders, P. Crews, and D. Drubin. 1997. High rates of actin turnover in budding yeast and roles for actin in establishment and maintenance of cell polarity revealed using the actin inhibitor latrunculin-A. *J. Cell Biol.* 137:399–416.

Balasubramanian, M., D. Helfman, and S. Hemmingsen. 1992. A new tropomyosin essential for cytokinesis in the fission yeast *S. pombe. Nature.* 360:84–87.

Ballou, C. 1990. Isolation, characterization, and properties of *Saccharomyces cerevisiae mnn* mutants with nonconditional protein glycosylation defects. *Methods Enzymol.* 185:440–470.

Belmont, L., and D. Drubin. 1998. The yeast V159N actin mutant reveals roles for actin dynamics in vivo. *J. Cell Biol.* 142:1289–1299.

Bender, A., and J. Pringle. 1989. Multi-copy suppression of the *cdc24* budding defect in yeast by *CDC42* and three newly identified genes including the ras-related gene *RSR1*. *Proc. Natl. Acad. Sci. USA.* 86:9976–9980.

Brennwald, P., and P. Novick. 1993. Interactions of three domains distinguishing the Ras-related GTP-binding proteins Ypt1 and Sec4. *Nature.* 360:560–563.

Bretscher, A., B. Drees, E. Harsay, D. Schott, and T. Wang. 1994. What are the basic functions of microfilaments? Insights from studies in budding yeast. *J. Cell Biol.* 126:821–825.

Brown, S. 1997. Myosins in yeast. *Curr. Opin. Cell Biol.* 9:44–48.

Cadwell, R., and G. Joyce. 1992. Randomization of genes by PCR mutagenesis. *PCR Methods and Applications.* 2:28–33.

Chant, J., and J. Pringle. 1995. Patterns of bud-site selection in the yeast *Saccharomyces cerevisiae. J. Cell Biol.* 129:751–765.

Drees, B., C. Brown, B. Barrell, and A. Bretscher. 1995. Tropomyosin is essential in yeast, yet the *TPM1* and *TPM2* products perform distinct functions. *J. Cell Biol.* 28:383–392.

Drubin, D., and W.J. Nelson. 1996. Origins of cell polarity. *Cell.* 84:335–344.

Dykstra, M. 1993. A Manual of Applied Techniques for Biological Electron Microscopy. Plenum Press, New York. 175–179.

Epp, J., and J. Chant. 1997. An IQGAP-related protein controls actin-ring formation and cytokinesis in yeast. *Curr. Biol.* 7:921–929.

Field, C., and R. Schekman. 1980. Localized secretion of acid-phosphatase reflects the pattern of cell growth in *Saccharomyces cerevisiae. J. Cell Biol.* 86: 123–128.

Finger, F., and P. Novick. 1998. Spatial regulation of exocytosis: lessons from yeast. *J. Cell Biol.* 142:609–612.

Finger, F., T. Hughes, and P. Novick. 1998. Sec3p is a spatial landmark for polarized secretion in budding yeast. *Cell.* 92:559–571.

Gassmann, M., P. Thömmes, T. Weiser, and U. Hübscher. 1990. Efficient production of chicken egg yolk antibodies against a conserved mammalian protein. *FASEB (Fed. Am. Soc. Exp. Biol.) J.* 4:2528–2532.

Geli, M.I., and H. Riezman. 1998. Endocytic internalization in yeast and animal cells: similar and different. *J. Cell Sci.* 111:1031–1037.

Goodson, H., B. Anderson, H. Warrick, L. Pon, and J. Spudich. 1996. Synthetic lethality screen identifies a novel yeast myosin I gene (*MYO5*): myosin I proteins are required for polarization of the actin cytoskeleton. *J. Cell Biol.* 133:1277–1291.

Goud, B., A. Salimen, N. Walworth, and P. Novick. 1988. A GTP-binding protein required for secretion rapidly associates with secretory vesicles and the plasma membrane in yeast. *Cell.* 53:753–768.

Govindan, B., R. Bowser, and P. Novick. 1995. The role of Myo2p, a yeast class V myosin, in vesicular transport. *J. Cell Biol.* 128:1055–1068.

Harsay, E., and A. Bretscher. 1995. Parallel secretory pathways to the cell surface in yeast. *J. Cell Biol.* 131:297–310.

Horvath, A., and H. Riezman. 1994. Rapid protein extraction from *Saccharomyces cerevisiae. Yeast.* 10:1305–1310.

Ito, H., Y. Fukuda, and A. Kimura. 1983. Transformation of intact yeast cells treated with alkali cations. *J. Bacteriol.* 153:163–168.

Johnson, D., and J. Pringle. 1990. Molecular characterization of *CDC42*, a *Saccharomyces cerevisiae* gene involved in the development of cell polarity. *J. Cell Biol.* 111:143–152.

Johnston, G., J. Prendergast, and R. Singer. 1991. The *Saccharomyces cerevisiae MYO2* gene encodes an essential myosin for vectorial transport of vesicles. *J. Cell Biol.* 113:539–551.

Kagami, M., A. Toh-e, and Y. Matsui. 1997. *SRO9*, a multisopy suppressor of the bud growth defect in the *Saccharomyces cerevisiae rho3*-deficient cells, shows strong genetic interactions with tropomyosin genes, suggesting its role in organization of the actin cytoskeleton. *Genetics.* 147:1003–1016.

Kaiser, C., and R. Schekman. 1990. Distinct sets of *SEC* genes govern vesicle formation and fusion early in the secretory pathway. *Cell.* 61:723–733.

Karpova, T., J. McNally, S. Moltz, and J. Cooper. 1998. Assembly and function of the actin cytoskeleton of yeast: relationships between cables and patches. *J. Cell Biol.* 142:1501–1517.

Keller, P., and K. Simons. 1997. Post-Golgi biosynthetic trafficking. *J. Cell Sci.* 110:3001–3009.

Laemmli, U. 1970. Cleavage of structural proteins during the assembly of the head of bacteriophage T_4. *Nature.* 227:680–685.

Lew, D., and S. Reed. 1995. A cell cycle checkpoint monitors cell morphogenesis in budding yeast. *J. Cell Biol.* 129:739–749.

Lillie, S., and S. Brown. 1994. Immunofluorescence localization of the unconventional myosin, Myo2p, and the putative kinesin-related protein, Smy1p, to the same regions of polarized growth in *Saccharomyces cerevisiae*. *J. Cell Biol.* 125:825–842.

Lippincott, J., and R. Li. 1998. Sequential assembly of myosin II, an IQGAP-like protein, and filamentous actin to a ring structure involved in budding yeast cytokinesis. *J. Cell Biol.* 140:355–366.

Liu, H., and A. Bretscher. 1989*a*. Purification of tropomyosin from *Saccharomyces cerevisiae* and identification of related proteins in *Schizosaccharomyces* and *Physarum*. *Proc. Natl. Acad. Sci. USA*. 86:90–93.

Liu, H., and A. Bretscher. 1989*b*. Disruption of the single tropomyosin gene in yeast results in the disappearance of actin cables from the cytoskeleton. *Cell.* 57:233–242.

Liu, H., and A. Bretscher. 1992. Characterization of *TPM1* disrupted yeast cells indicates an involvement of tropomyosin in directed vesicular transport. *J. Cell Biol.* 118:285–299.

McMillan, J., R. Sia, and D. Lew. 1998. A morphogenesis checkpoint monitors the actin cytoskeleton in yeast. *J. Cell Biol.* 142:1487–1499.

Mrsa, V., F. Klebl, and W. Tanner. 1993. Purification and characterization of the *Saccharomyces cerevisiae BGL2* gene product, a cell wall endo-β-1,3-glucanase. *J. Bacteriol.* 175:2102–2106.

Muhlrad, D., R. Hunter, and R. Parker. 1992. A rapid method for localized mutagenesis of yeast genes. *Yeast.* 8:79–82.

Novick, P., and R. Schekman. 1979. Secretion and cell-surface growth are blocked in a temperature-sensitive mutant of *Saccharomyces cerevisiae*. *Proc. Natl. Acad. Sci. USA*. 76:1858–1862.

Novick, P., and D. Botstein. 1985. Phenotypic analysis of temperature-sensitive yeast actin mutants. *Cell.* 40:405–416.

Novick, P., C. Field, and R. Schekman. 1980. Identification of 23 complementation groups required for post-translational events in the yeast secretory pathway. *Cell.* 21:205–215.

Pringle, J., R. Preston, A. Adams, T. Stearns, D. Drubin, B. Haarer, and E. Jones. 1989. Fluorescence microscopy methods for yeast. *Methods Cell Biol.* 31:357–435.

Riezman, H. 1985. Endocytosis in yeast: several of the yeast secretory mutants are defective in endocytosis. *Cell.* 40:1001–1009.

Sherman, F. 1991. Getting started with yeast. *Methods Enzymol.* 194:3–21.

Sikorski, R., and P. Hieter. 1989. A system of shuttle vectors and yeast host strains designed for efficient manipulation of DNA in *Saccharomyces cerevisiae*. *Genetics.* 122:19–27.

Tanaka, K., and Y. Takai. 1998. Control of reorganization of the actin cytoskeleton by Rho family small GTP-binding proteins in yeast. *Curr. Opin. Cell Biol.* 10:112–116.

TerBush, D., and P. Novick. 1995. Sec6, Sec8, and Sec15 are components of a multisubunit complex which localizes to small bud tips in *Saccharomyces cerevisiae*. *J. Cell Biol.* 130:299–312.

TerBush, D., T. Maurice, D. Roth, and P. Novick. 1996. The exocyst is a multiprotein complex required for exocytosis in *Saccharomyces cerevisiae. EMBO (Eur. Mol. Biol. Organ.) J.* 15:6483–6494.

Thacz, J., and J. Lampen. 1972. Wall replication in *Saccharomyces* species: use of fluorescein-conjugated concavalin-A to reveal the site of mannan insertion. *J. Gen. Microbiol.* 72:243–247.

Thacz, J., and J. Lampen. 1973. Surface distribution of invertase on growing *Saccharomyces cerevisiae*. *J. Bacteriol.* 113:1073–1075.

Waddle, J., T. Karpova, R. Waterston, and J. Cooper. 1996. Movement of cortical actin patches in yeast. *J. Cell Biol.* 132:861–870.

Walch-Solimena, C., R. Collins, and P. Novick. 1997. Sec2p mediates nucleotide exchange on Sec4p and is involved in polarized delivery of post-Golgi vesicles. *J. Cell Biol.* 137:1495–1509.

Wendland, B., S. Emr, and H. Riezman. 1998. Protein traffic in the yeast endocytic and vacuolar protein sorting pathways. *Curr. Opin. Cell Biol.* 10: 513–522.

Zheng, Y., R. Cerione, and A. Bender. 1993. Control of the yeast bud-site assembly GTPase Cdc42: catalysis of guanine nucleotide exchange by Cdc24 and stimulation of GTPase activity by Bem3. *J. Biol. Chem.* 269:2369–2372.